# Free-Radical Ring Closure to Conformationally Locked α-L-Carba-LNAs and Synthesis of Their Oligos: Nuclease Stability, Target RNA Specificity, and Elicitation of RNase H

Qing Li, Fengfeng Yuan, Chuanzheng Zhou, Oleksandr Plashkevych, and Jyoti Chattopadhyaya*

Program of Bioorganic Chemistry, Institution of Cell and Molecular Biology, Box 581, Biomedical Center, Uppsala University, SE-751 23 Uppsala, Sweden

jyoti@boc.uu.se
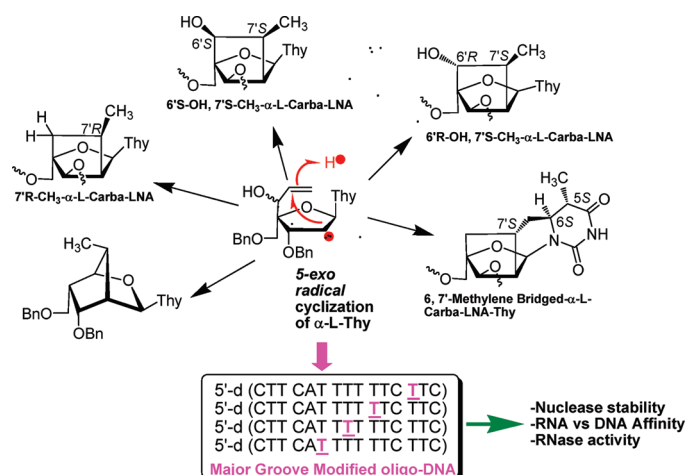
A new class of conformationally constrained nucleosides, α-L-_ribo_-carbocyclic LNA thymidine (α-L-carba-LNA-T, LNA is an abbreviation of locked nucleic acid) analogues and a novel "double-locked" α-L-_ribo_-configured tetracyclic thymidine (6,7′-methylene-bridged-α-L-carba-LNA-T) in which both the sugar puckering and glycosidic torsion are simultaneously constrained, have been synthesized through a key step involving 5-_exo_ free-radical intramolecular cyclization. These α-L-carba-LNA analogues have been subsequently transformed to corresponding phosphoramidites and incorporated into isosequential antisense oligonucleotides (AONs), which have then been examined for the thermal denaturation of their duplexes, nuclease stability, and RNase H recruitment capabilities. Introduction of a single 6′,7′-substituted α-L-carba-LNA-T modification in the AON strand of AON/RNA heteroduplex led to T_m reduction by 2−3 °C as compared to the native heteroduplex, whereas the parent 2′-oxa-α-L-LNA-T modification at the identical position in the AON strand has been found to lead to an increase in the T_m by 3−5 °C. This suggests that the 6′ and 7′ substitutions lead to much reduced thermal stability for the modified heteroduplex, especially the hydrophobic 7′-methyl on α-L-carba-LNA, which is located in the major groove of the duplex. All of the AONs incorporating 6′,7′-substituted α-L-carba-LNA-T have, however, showed considerably improved nuclease stability toward 3′-exonuclease (SVPDE) and in human blood serum compared to the 2′-oxa-α-L-LNA-T incorporated AONs. The hybrid duplexes that are formed by 6′,7′-substituted α-L-carba-LNA-T-modified AONs with complementary RNA have been found to recruit RNase H with higher efficiency than those of the $β$-D-LNA-T or $β$-D-carba-LNA-T-modified counterparts. These greatly improved nuclease resistances and efficient RNase H recruitment capabilities elevate the α-L-carba-LNA-modified nucleotides into a new class of locked nucleic acids for potential RNA targeting therapeutics.

Introduction

Among the varieties of gene silencing technologies, the antisense strategy[1] and RNA interference[2] are considered to be extremely potent in terms of ensuring complete target mRNA breakdown. During the last couple of decades, exploration and examination of novel chemically modified oligonucleotides that act as potent and selective therapeutic agents have gained momentum and have led to the development of analogues which have good pharmacokinetics and minimum toxicity. In general, there are three main types of possible chemical modifications of native nucleotides, and each involves modification of either sugar, phosphodiester linkage, or nucleobase.[3]

In recent years, a variety of conformationally constrained nucleotides[4–6] have been synthesized and incorporated into antisense oligonucleotides (AONs) and/or siRNAs for in vitro biological studies. One particular class of compounds, so-called locked nucleic acid (LNA,[7,8] also called BNA,[9,10] BNA is the abbreviation of bridged nucleic acid) containing a methylene linkage between the 2′-oxygen and 4′-carbon of the ribose ring, has attracted extensive interest due to their remarkable hybridization properties.[8] The excellent thermodynamic features of LNA stimulated synthesis of a number of other North-type conformationally constrained nucleoside analogues, such as amino-LNA,[11] β-bicyclonucleoside,[12] C6′-substituted LNA,[13,14] BNA^{COC},[15] BNA^{NC},[16,17] 2′-O,4′-C-ethylene-bridged nucleic acid (ENA),[18,19] aza-ENA,[20–22] carba-ENA[23,24] etc. All of these locked nucleoside-modified AONs have shown much better

antisense properties, such as RNA affinity, nuclease resistance, and RNase H elicitation, as compared to that of the native counterpart. Some of these locked nucleotides have been tested for siRNA action and have shown remarkable silencing efficiency.[25,26]

Recently, carba-LNA, carba-ENA, C6′,C7′-substituted carba-LNAs, and C6′,C8′-substituted carba-ENAs have been synthesized by our group through a key step involving intramolecular free-radical ring closure.[27–32] The striking feature of carba-LNA and carba-ENA derivatives is that they render much better nuclease resistance for modified AONs than LNA.[32] The carbocyclic ring of carba-LNA and carba-ENA also provides an effective handle for engineering new types of modifications in the minor groove, which can significantly modulate important antisense properties such as target RNA affinity, nuclease resistance without impairing their RNase H recruitment capabilities.

Another intriguing class of conformationally constrained nucleoside, α-L-LNA, is a diastereomer of LNA[7,8] (referred to as β-D-LNA further in the text in order to distinguish from α-L-LNA). The α-L-LNA has also been synthesized by Wengel et al.[33–40] Thermal stability of α-L-LNA-modified AON with complementary nucleic acid targets was found to be comparable to that of LNA-containing counterparts. Moreover, it has been shown that the α-L-LNA modification renders better nuclease resistance compared to LNA modification.[36] In vitro and in vivo experiments showed that α-L-LNA-modified AONs retain the ability of RNase H elicitation and exhibit even higher gene knockdown efficacy than LNA-modified counterparts.[41,42]

(1) Crooke, S. T. *Annu. Rev. Med.* **2004**, *55*, 61–95.

(2) Novina, C. D.; Sharp, P. A. *Nature* **2004**, *430*, 161–164.

(3) Freier, S. M.; Altmann, K. H. *Nucleic Acids Res.* **1997**, *25*, 4429–4435.

(4) Zhou, C.; Chattopadhyaya, J. *Curr. Opin. Drug Discovery Dev.* **2009**, *12*, 876–898.

(5) Herdewijn, P. *Liebigs Ann.* **1996**, 1337–1348.

(6) Mathe, C; Perigaud, C. *Eur. J. Org. Chem.* **2008**, 1489–1505.

(7) Singh, S. K.; Nielsen, P.; Koshkin, A. A.; Wengel, J. *Chem. Commun.* **1997**, 1643–1644.

(8) Koshkin, A. A.; Singh, S. K.; Nielsen, P.; Rajwanshi, V. K.; Kumar, R.; Meldgaard, M.; Olsen, C. E.; Wengel, J. *Tetrahedron* **1998**, *54*, 3607–3630.

(9) Obika, S.; Nanbu, D.; Hari, Y.; Morio, K.; In, Y.; Ishida, T.; Imanishi, T. *Tetrahedron Lett.* **1997**, *38*, 8735–8738.

(10) Obika, S.; Nanbu, D.; Hari, Y.; Andoh, J.; Morio, K.; Doi, T.; Imanishi, T. *Tetrahedron Lett.* **1998**, *39*, 5401–5404.

(11) Singh, S. K.; Kumar, R.; Wengel, J. *J. Org. Chem.* **1998**, *63*, 10035–10039.

(12) Wang, G.; Girardet, J. L.; Gunic, E. *Tetrahedron* **1999**, *55*, 7707–7724.

(13) Enderlin, G.; Nielsen, P. *J. Org. Chem.* **2008**, *73*, 6891–6894.

(14) Seth, P. P.; Vasquez, G.; Allerson, C. A.; Berdeja, A.; Gaus, H.; Kinberger, G. A.; Prakash, T. P.; Migawa, M. T.; Bhat, B.; Swayze, E. E. *J. Org. Chem.* **2010**, *75*, 1569–1581.

(15) Hari, Y.; Obika, S.; Ohnishi, R.; Eguchi, K.; Osaki, T.; Ohishi, H.; Imanishi, T. *Bioorg. Med. Chem.* **2006**, *14*, 1029–1038.

(16) Rahman, S. M. A.; Seki, S.; Obika, S.; Yoshikawa, H.; Miyashita, K.; Imanishi, T. *J. Am. Chem. Soc.* **2008**, *130*, 4886–4896.

(17) Prakash, T. P.; Siwkowski, A.; Allerson, C. A.; Migawa, M. T.; Lee, S.; Gaus, H. J.; Black, C.; Seth, P. P.; Swayze, E. E.; Bhat, B. *J. Med. Chem.* **2010**, *53*, 1636–1650.

(18) Morita, K.; Takagi, M.; Hasegawa, C.; Kaneko, M.; Tsutsumi, S.; Sone, J.; Ishikawa, T.; Imanishi, T.; Koizumi, M. *Bioorg. Med. Chem.* **2003**, *11*, 2211–2226.

(19) Morita, K.; Hasegawa, C.; Kaneko, M.; Tsutsumi, S.; Sone, J.; Ishikawa, T.; Imanishi, T.; Koizumi, M. *Bioorg. Med. Chem. Lett.* **2002**, *12*, 73–76.

(20) Varghese, O. P.; Barman, J.; Pathmairi, W.; Plashkevych, O.; Honcharenko, D.; Chattopadhyaya, J. *J. Am. Chem. Soc.* **2006**, *128*, 15173–15187.

(21) Honcharenko, D.; Barman, J.; Varghese, O. P.; Chattopadhyaya, J. *Biochemistry* **2007**, *46*, 5635–5646.

(22) Honcharenko, D.; Zhou, C.; Chattopadhyaya, J. *J. Org. Chem.* **2008**, *73*, 2829–2842.

(23) Albæk, N.; Petersen, M.; Nielsen, P. *J. Org. Chem.* **2006**, *71*, 7731–7740.

(24) Kumar, S.; Hansen, M. H.; Albæk, N.; Steffansen, S. I.; Petersen, M.; Nielsen, P. *J. Org. Chem.* **2009**, *74*, 6756–6769.

(25) Nauwelaerts, K.; Fisher, M.; Froeyen, M.; Lescrinier, E.; Van Aerschot, A.; Xu, D.; Delong, R.; Kang, H.; Juliano, R. L.; Herdewijn, P. *J. Am. Chem. Soc.* **2007**, *129*, 9340–9348.

(26) Bramsen, J. B.; Laursen, M. B.; Nielsen, A. F.; Hansen, T. B.; Bus, C.; Langkjær, N.; Babu, B. R.; Højland, T.; Abramov, M.; Van Aerschot, A.; Odadzic, D.; Smicius, R.; Haas, J.; Andree, C.; Barman, J.; Wenska, M.; Srivastava, P.; Zhou, C.; Honcharenko, D.; Hess, S.; Muller, E.; Bobkov, G. V.; Mikhailov, S. N.; Fava, E.; Meyer, T. F.; Chattopadhyaya, J.; Zerial, M.; Engels, J. W.; Herdewijn, P.; Wengel, J.; Kjems, J. *Nucleic Acids Res.* **2009**, *37*, 2867–2881.

(27) Srivastava, P.; Barman, J.; Pathmasiri, W.; Plashkevych, O.; Wenska, M.; Chattopadhyaya, J. *J. Am. Chem. Soc.* **2007**, *129*, 8362–8379.

(28) Zhou, C.; Liu, Y.; Andaloussi, M.; Badgujar, N.; Plashkevych, O.; Chattopadhyaya, J. *J. Org. Chem.* **2009**, *74*, 118–134.

(29) Xu, J.; Liu, Y.; Dupouy, C.; Chattopadhyaya, J. *J. Org. Chem.* **2009**, *74*, 6534–6554.

(30) Zhou, C.; Plashkevych, O.; Chattopadhyaya, J. *Org. Biomol. Chem.* **2008**, *6*, 4627–4633.

(31) Zhou, C.; Plashkevych, O.; Chattopadhyaya, J. *J. Org. Chem.* **2009**, *74*, 3248–3265.

(32) Zhou, C.; Chattopadhyaya, J. *J. Org. Chem.* **2010**, *75*, 2341–2349.

(33) Rajwanshi, V. K.; Hakansson, A. E.; Dahl, B. M.; Wengel, J. *Chem. Commun.* **1999**, 1395–1396.

(34) Rajwanshi, V. K.; Hakansson, A. E.; Kumar, R.; Wengel, J. *Chem. Commun.* **1999**, 2073–2074.

(35) Hakansson, A. E.; Koshkin, A. A.; Sørensen, M. D.; Wengel, J. *J. Org. Chem.* **2000**, *65*, 5161–5166.

(36) Sørensen, M. D.; Kværnø, L.; Bryld, T.; Hakansson, A. E.; Verbeure, B.; Gaubert, G.; Herdewijn, P.; Wengel, J. *J. Am. Chem. Soc.* **2002**, *124*, 2164–2176.

(37) Rajwanshi, V. K.; Hakansson, A. E.; Sørensen, M. D.; Pitsch, S.; Singh, S. K.; Kumar, R.; Nielsen, P.; Wengel, J. *Angew. Chem., Int. Ed.* **2000**, *39*, 1656–1659.

(38) Petersen, M.; Hakansson, A. E.; Wengel, J.; Jacobsen, J. P. *J. Am. Chem. Soc.* **2001**, *123*, 7431–7432.

(39) Kumar, T. S.; Madsen, A. S.; Wengel, J.; Hrdlicka, P. J. *J. Org. Chem.* **2006**, *71*, 4188–4201.

(40) Kumar, T. S.; Madsen, A. S.; Østergaard, M. E.; Sau, S. P.; Wengel, J.; Hrdlicka, P. J. *J. Org. Chem.* **2009**, *74*, 1070–1081.

(41) Fluiter, K.; Frieden, M.; Vreijling, J.; Rosenbohm, C.; De Wissel, M. B.; Christensen, S. M.; Koch, T.; Ørum, H.; Baas, F. *ChemBioChem* **2005**, *6*, 1104–1109.

(42) Frieden, M.; Christensen, S. M.; Mikkelsen, N. D.; Rosenbohm, C.; Thrue, C. A.; Westergaard, M.; Hansen, H. F.; Ørum, H.; Koch, T. *Nucleic Acids Res.* **2003**, *31*, 6363–6372.
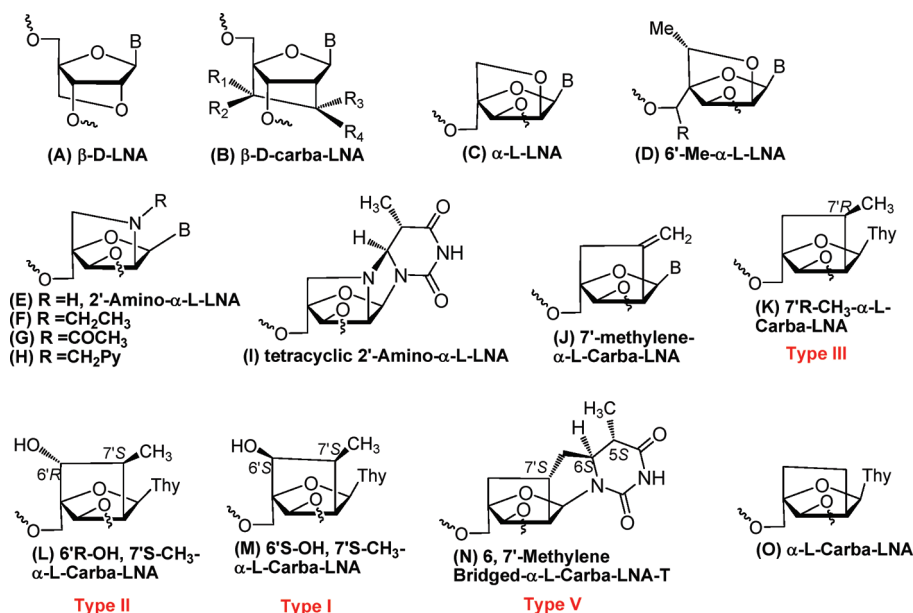
FIGURE 1. Structures of β-D-LNA (A),[7−9] β-D-carba-LNA (B),[27−29] α-L-LNA (C),[33−37] 6'-Me-α-L-LNA (D),[44] 2'-amino-α-L-LNA (E)[39] and derivatives (F−H),[40] tetracyclic 2'-amino-α-L-LNA (I),[39] 7'-methylene-α-L-carba-LNA (J): This nucleoside was reported in a recent patent,[43] but it was not characterized, not even partially, by either ^{1}H or ^{13}C NMR. Instead, only ^{31}P NMR of the corresponding phosphoramidite was supplied, which in fact could be the same for any nucleoside phosphoramidite). 6',7'-Substituted α-L-carba-LNA derivatives (K−M), along with a novel double-locked α-L-carba-LNA analogue: 6,7'-methylene-bridged α-L-carba-LNA-T (N).

The striking biochemical features of α-L-LNA prompted us and others[43,44] to synthesize α-L-*ribo*-carba-LNA, in which a methylene group replaces the 2'-oxygen of α-L-LNA yielding a 2',4'-carbocyclic locked ring. Unlike the 2',4'-carbocycle locked ring in carba-LNA (referred to as β-D-carba-LNA further in the text in order to distinguish from α-L-carba-LNA), which is located in the minor groove of AON/RNA duplexes, the 2',4'-carbocyclic ring in α-L-carba-LNA is located in the major groove of AON/RNA duplexes (see Figure SII 41 and 42 in Supporting Information). Hence C6'/7'-substituted α-L-carba-LNAs are also very good models to study how different substitutions in the major groove modulate biophysical and biochemical properties of AON/RNA duplexes. Herein, we report a viable synthetic route to 6',7'-substituted α-L-carba-LNA thymidine derivatives (Figure 1K−M) along with a so-called "double-locked" tetracyclic α-L-carba-LNA thymidine (Figure 1N) formed by the intramolecular addition of methylene free radical to thymine nucleobase. In order to evaluate α-L-carba-LNA nucleosides' potential for therapeutic applications, all of these modified nucleotides have subsequently been introduced into AONs to study thermal stabilities of their duplexes with complementary RNA or DNA, as well as the 3'-exonuclease resistances, human blood serum stabilities, and RNase H recruitment capabilities in comparison with that of α-L-LNA and β-D-carba-LNA-modified counterparts.

Results and Discussion

1. Synthesis of Diastereomerically Pure 6',7'-Substituted α-L-Carba-LNAs and 6,7'-Methylene-Bridged α-L-Carba-LNA-T. The synthetic route to the 6',7'-substituted α-L-carba-LNA thymidine phosphoramidites **16a**, **16b**, and **16c** is shown in Schemes 1−3. The synthesis started from the known nucleoside 3,5-di-*O*-benzyl-4-hydroxylmethyl-1,2-*O*-isopropylidene-β-L-ribofuranose **1**,[45] which was oxidized to the corresponding aldehyde **2** through Swern oxidation. The crude aldehyde was subjected to Grignard reaction with vinylmagnesium bromide to afford two pure diastereomers **3a** (6'R-OH) and **3b** (6'S-OH) in moderate yields (32% for **3a**, 29% for **3b** in two steps). The configuration at C6' could not be confirmed by nuclear Overhauser effect (NOE) experiment at this stage. This could, however, be confirmed after the free-radical cyclization step (see section 2 for discussion on NMR characterization), which subsequently showed the C6'-*R* and -*S* stereochemistry for **3a** and **3b**, respectively. Acetylation of **3a** with a mixture of acetic anhydride, acetic acid, and triflic acid gave the corresponding triacetate **4a** as an anomeric mixture. The crude triacetate **4a** was then subjected to a modified Vorbrüggen reaction[46] involving *in situ* silylation of the thymine and subsequent trimethylsilyl triflate mediated coupling to give exclusive α-L-ribofuranosyl thymine derivative **5a**. Deacetylation of **5a** using 30% methylamine in ethanol at room temperature overnight gave compound **6a** quantitatively, which was treated with phenyl chlorothioformate to afford the key free-radical precursor **7a** (6'-*R*) in high yield (86%) without any formation of 6'-*O*-phenoxythiocarbonyl (PTC) product even when 2.5 equiv of phenyl chlorothioformate was used. We have also similarly synthesized the second free-radical precursor **7b** (6'-*S*) from **3b** (6'-*S*) (Scheme 1).

The free-radical cyclization was carried out in refluxing anhydrous toluene with Bu₃SnH, using AIBN as the initiator, which was added dropwise in order to avoid the side reactions. Cyclization of **7a** (6'-*R*) took place with high stereoselectivity

(43) Seth, P. P.; Swayze, E. E. Patent WO2009/067647 A1.
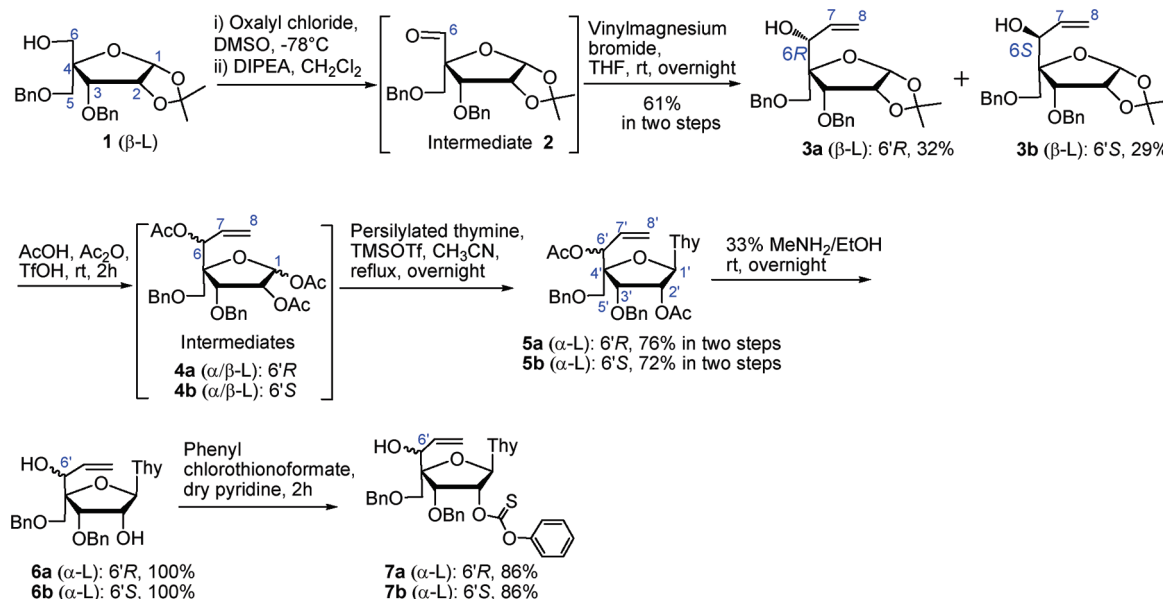(44) Seth, P. P.; Swayze, E. E. Patent WO2010/036698 A1.

(45) Nacro, K.; Lee, J.; Barchi, J. J.; Lewin, N. E.; Blumberg, P. M.; Marquez, V. E. *Tetrahedron* **2002**, *58*, 5335–5345.
(46) Vorbrüggen, H; Krolikiewicz, K.; Bennua, B. *Chem. Ber.* **1981**, *114*, 1234–1255.
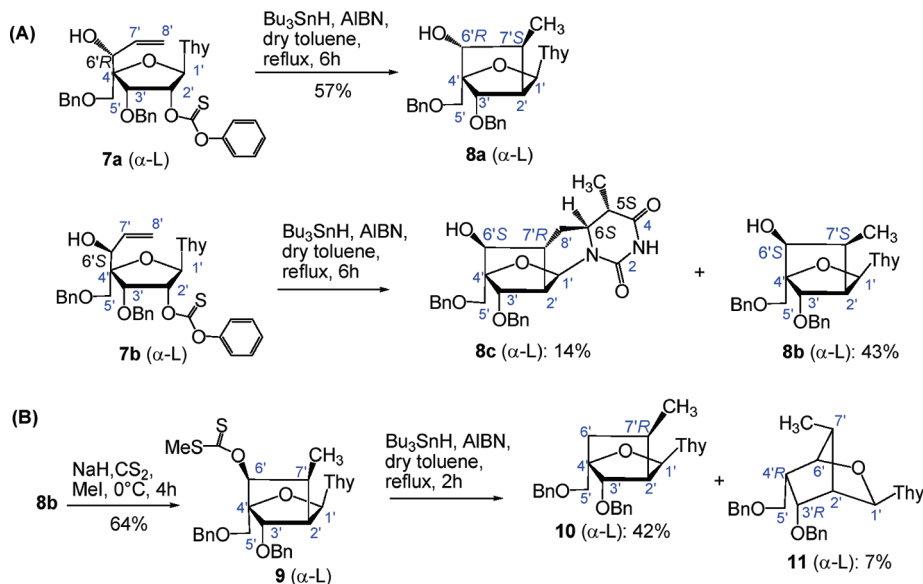
SCHEME 1

SCHEME 2

to give α-L-carba-LNA nucleoside **8a** (6′R-OH,7′S-CH$_3$) in good yield (57%, Scheme 2). Under an identical condition, cyclization of **7b** (6′-S), on the other hand, gave α-L-carba-LNA nucleoside **8b** (6′S-OH,7′S-CH$_3$) in 43% yield along with an unexpected product **8c** in a 14% yield (Scheme 2). The mechanism of the free-radical cyclization reaction for the formation of **8a**, **8b**, and **8c** will be discussed in section 3.

In an effort to remove the 6′S-OH in compound **8b** by radical deoxygenation strategy, we attempted to esterify the 6′-OH using phenyl chlorothioformate but failed. This suggested that 6′S-OH is much more inert than the 2′-OH group in the pentose sugar moiety. Transformation of OH to (methylthio)thiocarbonate has been proven to be an efficient

solution to remove an inert hydroxyl group by radical deoxygenation.[47] Thus, **8b** was treated with CS$_2$ and MeI along with NaH as a base at 0 °C for 4 h, giving the radical precursor **9** in 64% yield. Then, compound **9** was subjected to the standard Barton−McCombie deoxygenation[48] in the presence of Bu$_3$SnH and AIBN to furnish 7′S-CH$_3$-α-L-carba-LNA nucleoside **10** in 42% yield plus an unexpected bicyclo-[2.2.1]-2′,6′-methylene-bridged hexopyranosyl nucleoside **11** in 7% yield (Scheme 2). The radical rearrangement process[49] that leads to **11** will be discussed in section 3.

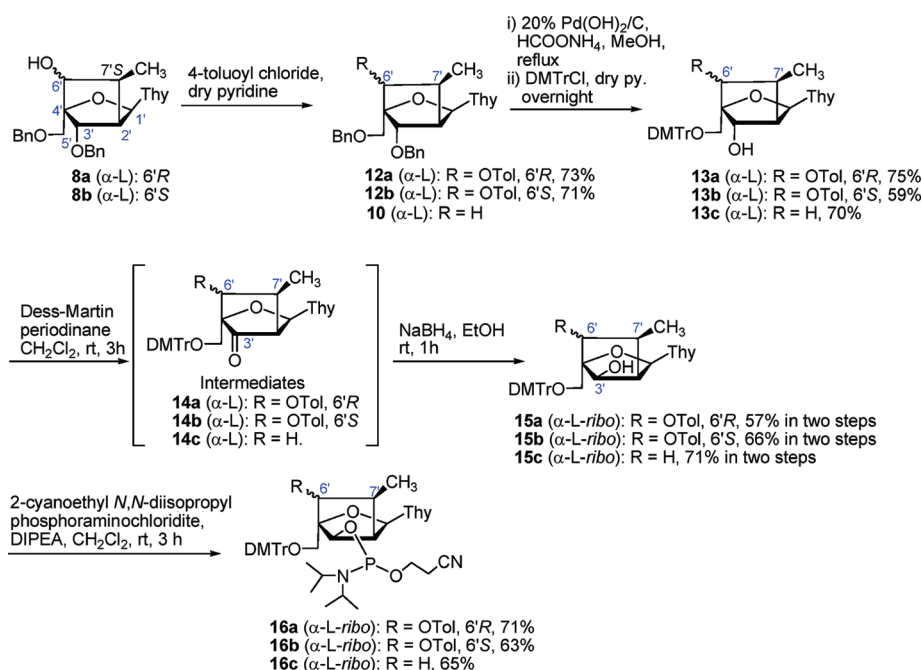In order to convert **8a/b** to the corresponding phosphoramidites for solid-supported DNA synthesis, the 6′-OH

(47) Mereyala, H. B.; Pola, P. *Synth. Commun.* **2002**, *32*, 2453–2458.

(48) Barton, D. H. R.; McCombie, S. W. *J. Chem. Soc., Perkin Trans. 1* **1975**, *16*, 1574–1585.

(49) Zhou, C.; Plashkevych, O.; Liu, Y.; Badgujar, N.; Chattopadhyaya, J. *Heterocycles* **2009**, *78*, 1715–1728.

SCHEME 3

group of **8a** and **8b** must be protected (Scheme 3). Thus compounds **8a** and **8b** were treated with *p*-toluoyl chloride in dry pyridine to give compounds **12a** and **12b** in 73 and 71% yield, respectively. Then compounds **12a**, **12b**, and **10** were subjected to debenzylation using 20% Pd(OH)$_2$/C and ammonium formate followed by selectively protecting the 5'-OH with DMTr, giving **13a**, **13b**, and **13c**, respectively. It should be noted that debenzylation of **12b** should be limited to 20 min, and a prolongation of reaction time led to cleavage of a 6'-*O*-(*p*-toluoyl) group by the attack of the primary 5'-OH group.[28] In order to invert the configuration of 3'-OH, compounds **13a**, **13b**, and **13c** were oxidized with Dess−Martin periodinane[50−52] followed by the reduction with sodium borohydride in ethanol to give **15a**, **15b**, and **15c**, respectively, in 57−71% yields. The complete inversion of 3'-OH is facilitated by the carbocyclic ring and 7'-Me on the top side of the furan sugar, which leads to significant steric hindrance, thus promoting exclusive attack of the hydride from the bottom of the furanose sugar ring. Compounds **15a**, **15b**, and **15c** were then phosphitylated with 2-cyanoethyl-*N*,*N*-diisopropylphosphoraminochloridite under standard conditions,[27−29] giving phosphoramidites **16a**, **16b**, and **16c**, respectively, as a diastereomeric mixture in 63−71% yield.

The unexpected product **8c** obtained during free-radical cyclization of **7b** was also transformed to corresponding phosphoramidite **22** (Scheme 4). Thus, **8c** was treated with CS$_2$, MeI, and NaH, leading to the successful acquisition of radical precursor **17** in 69% yield, followed by the Barton−McCombie deoxygenation[48] affording product **18** in high yield (95%). Debenzylation of **18** using 20% Pd(OH)$_2$/C and ammonium formate, followed by 5'-*O*-dimethoxytritylation smoothly gave **19** (72% in two steps). Since oxidation of **19** with Dess−Martin periodinane failed to give the corresponding ketone, another

mild oxidizing reagent known as TPAP (tetra-*n*-propylammonium perruthenate) was used.[53] Therefore, compound **19** was treated with catalytic amount of TPAP along with the stoichiometric oxidant NMO (*N*-methylmorpholine-*N*-oxide) at room temperature to afford **20**, which was directly subjected to the reduction with sodium borohydride at −20 °C, giving products **21** (22% in two steps) plus recovery of starting material **19** (19% in two steps). Subsequently, the phosphitylation of **21** was performed with 2-cyanoethyl *N*,*N*-diisopropylphosphoraminochloridite under standard conditions[27−29] to furnish **22** (73% yield) as a diastereomeric mixture.

2. NMR Characterization of Key Intermediates Involved in the Synthesis of α-L-Carba-LNA Analogues. All of the key carbocyclic nucleoside intermediates have been characterized by ^{1}H, ^{13}C, COSY, ^{1}H−^{13}C HMQC, long-range ^{1}H−^{13}C correlation (HMBC) NMR experiments as well as by mass spectroscopy (see Supporting Information).

The formation of bicyclic systems in compounds **8a**, **8b**, **11**, and the tetracyclic system in compound **8c** was confirmed by HMBC and COSY experiments (discussed in details in part II of Supporting Information).

The orientation of substituents in the carbocyclic moiety of compound **8a** and **8b** was determined by 1D NOE experiments (Figure 2) as well as from the vicinal coupling constants evaluation. For compound **8a**, irradiation of H6 of thymine led to NOE enhancement for H7' (2.6%) ($d_{\text{H6−H7'}} \approx$ 2.5 Å) and for 6'-OH (0.9%) ($d_{\text{H6−6'-OH}} \approx 3.2$ Å), but none for 7'-CH$_3$ and H6' ($d_{\text{H6−7'-CH}_3} \approx 4.2$ Å, $d_{\text{H6−H6'}} \approx 4.6$ Å), whereas irradiation of 7'-CH$_3$ led to NOE enhancement for H6' (1.7%) ($d_{\text{H6'-7'-CH}_3} \approx 2.5$ Å) and H3' (1.7%) ($d_{\text{H3'-7'-CH}_3} \approx$ 2.4 Å), but none for 6'-OH ($d_{\text{7'-CH}_3-6'-OH} \approx 3.9$ Å), strongly suggesting that C6' is in 6'*R* configuration, and C7' is in 7'*S* configuration. In addition, the *trans* disposition of H6' and H7' was also in agreement with the small coupling constant
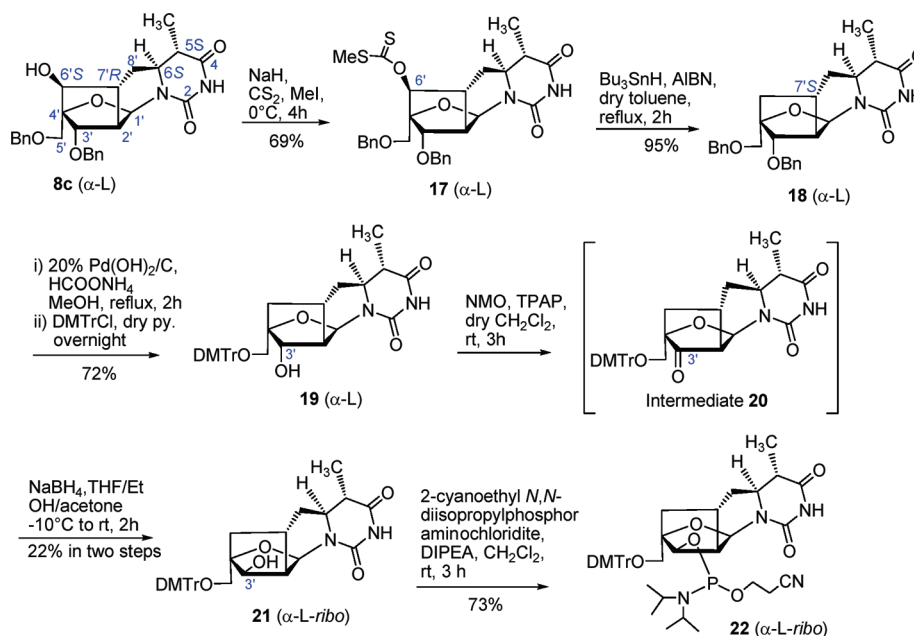
(50) Bose, D. S.; Narsaiah, A. V. *Synth. Commun.* **1999**, *29*, 937−941.

(51) Chaudhari, S. S.; Akamanchi, K. G. *Tetrahedron Lett.* **1998**, *39*, 3909−3912.

(52) Chaudhari, S. S.; Akamanchi, K. G. *Synthesis* **1998**, *5*, 760−764.

(53) Ley, S. V.; Norman, J.; Griffith, W. P.; Marsden, S. P. *Synthesis* **1994**, *7*, 639−666.

SCHEME 4

NaH, CS₂, MeI, 0 °C, 4h — 69%

8c (α-L)

MeS

17 (α-L)

Bu₃SnH, AIBN, dry toluene, reflux, 2h — 95%

18 (α-L)

i) 20% Pd(OH)₂/C, HCOONH₄ MeOH, reflux, 2h
ii) DMTrCl, dry py. overnight — 72%

19 (α-L)

NMO, TPAP, dry CH₂Cl₂, rt, 3h

Intermediate 20

NaBH₄, THF/EtOH/acetone −10 °C to rt, 2h — 22% in two steps

21 (α-L-*ribo*)

2-cyanoethyl *N,N*-diisopropylphosphoraminochloridite, DIPEA, CH₂Cl₂, rt, 3 h — 73%

22 (α-L-*ribo*)

for $^3J_{6',7'}$ (3.6 Hz, hence dihedral angle H6′−C6′−C7′−H7′ ≈ 232° according to Karplus equation). As for compound **8b**, irradiation of H6 of the thymine group led to NOE enhancement for H7′ (1.4%) ($d_{H6−H7'}$ ≈ 2.8 Å) and H6′ (2.7%) ($d_{H6−H7'}$ ≈ 2.5 Å), but none for 7′-CH₃ and 6′-OH ($d_{H6−7'-CH_3}$ ≈ 4.3 Å, $d_{H6−6'-OH}$ ≈ 4.4 Å), whereas irradiation of 7′-CH₃ leads to NOE enhancement for H3′ (1.6%) ($d_{H3'-7'-CH_3}$ ≈ 2.4 Å), but none for H6′ ($d_{H6'-7'-CH_3}$ ≈ 3.8 Å), suggesting that C6′ is in 6′S configuration, and C7′ is in 7′S configuration. Furthermore, the large coupling constant for $^3J_{6',7'}$ (8.5 Hz) corresponding to the dihedral angle of H6′−C6′−C7′−H7′ ≈ 26° also suggested a *cis* disposition of H6′ and H7′ in **8b**.

The stereochemistry of compound **11** was also determined by 1D NOE experiment (Figure 2). Therefore, selective irradiation of H4′ led to distinct NOE enhancement for H3′ (3.8%) ($d_{H3'-H4'}$ ≈ 2.3 Å), and irradiation of 7′-CH₃ led to NOE enhancement for H3′ (1.2%) ($d_{H3'-7'-CH_3}$ ≈ 2.4 Å) and H4′ (1.4%) ($d_{H4'-7'-CH_3}$ ≈ 2.4 Å), respectively, which suggested that H3′ and H4′ are *cis* oriented and they are on the same face as that of 7′-CH₃. The observation that irradiation of H1′ led to NOE enhancement for H5′, 5″ (1.1%) ($d_{H1'-H5',5''}$ ≈ 2.8 Å) but none for H3′ ($d_{H1'-H3'}$ ≈ 3.7 Å) and H4′ ($d_{H1'-H4'}$ ≈ 4.2 Å) suggested that H5′, 5″ are located on the face close to H1′. Hence, both and C3′ and C4′ are in *R* configuration for compound **11** (Figure 2).

For compound **8c**, in which four new chiral centers have been formed during a single free-radical cyclization step, the configuration of every chiral center was also well determined by 1D NOE experiments (see Figure 2). Selective irradiation of H6 in the thymine moiety led to strong NOE enhancement for H6′ (4.9%) ($d_{H6−H6'}$ ≈ 2.3 Å) and H8′ (2.4%) ($d_{H6−H8'}$ ≈ 2.4 Å), but none for 6′-OH and H7′ ($d_{H6−6'-OH}$ ≈ 4.1 Å, $d_{H6−H7'}$ ≈ 3.8 Å), unequivocally suggesting that C6′ is in 6′S configuration, C7′ is in 7′S configuration, and C6 is in 6S configuration, respectively. The *trans* disposition of H6′ and H7′ was also consistent with the coupling constant ($^3J_{6',7'}$ = 2.0 Hz, with dihedral angle H6′−C6′−C7′−H7′ ≈ 116°).

In addition, selective irradiation of H8″ of **19** (having the same carbon skeleton as **8c**) led to strong NOE enhancement for H5 (5.2%) ($d_{H5−H8''}$ ≈ 2.3 Å) and for H2′ (1.2%) ($d_{H2'−H8''}$ ≈ 2.8 Å), but none for 5-CH₃ group ($d_{5-CH_3−H8''}$ ≈ 3.8 Å), suggesting that C5 is in 5S configuration.

The configuration of 3′-OH in compounds **15a/b/c** and **21** was determined by 1D NOE experiment. Irradiation of H3′ showed 1.3, 0.6, and 0.5% NOE enhancements for H1′ ($d_{H1'−H3'}$ ≈ 2.3 Å), H2′ ($d_{H2'−H3'}$ ≈ 2.7 Å), and H5′, respectively, in compound **15a** (Figure SII.12 in Supporting Information), 3.2 and 1.9% NOE enhancements for H1′ and H5′, respectively, in compound **21** (Figure SII.11). Irradiation of H1′ led to 1.7 and 1.2% enhancement for H2′ ($d_{H1'−H2'}$ ≈ 2.3 Å) and H3′ ($d_{H1'−H3'}$ ≈ 2.5 Å), respectively, in **15b** (Figure SII.13) and 2.5 and 2.0% NOE enhancement for H2′ and H3′, respectively, in compound **15c** (Figure SII.14). These observations thus unequivocally indicated that 3′-OH's are in pseudoequatorial positions, while H3′ and H1′ are in pseudoaxial positions in compounds **15a/b/c** and **21**.

3. Mechanism of the Free-Radical Cyclization Reaction and Radical Rearrangement. It is known[54,55] that the 5-hexenyl intramolecular ring-closure reaction undergoes preferentially 1,5-ring closure (*exo* mode) over 1,6-ring closure (*endo* mode), yielding the thermodynamically less stable 5-*exo*-cyclization product.[53,54] The previous studies of 5-hexenyl and 6-heptenyl cyclization of the substituted β-D-carba-LNA and β-D-carba-ENA analogues in our lab have also suggested that the formation of bicyclic product is going predominantly via *exo* mode ring closure over *endo* mode.[27−29] After treatment of **7a** with Bu₃SnH and AIBN, the C2′ radical is supposed to be generated (TS1 in Scheme 5A), which should be capable of attacking the C=C double bond from both the "top" and "bottom" faces by the 5-*exo* cyclization pathway, resulting into two plausible intermediates, TS2 and TS3 (see Scheme 5A). The optimized structures have shown that in the TS2 state, the thymine moiety,

(54) Beckwith, A. L. J.; Schiesser, C. H. *Tetrahedron* **1985**, *41*, 3925−3941.
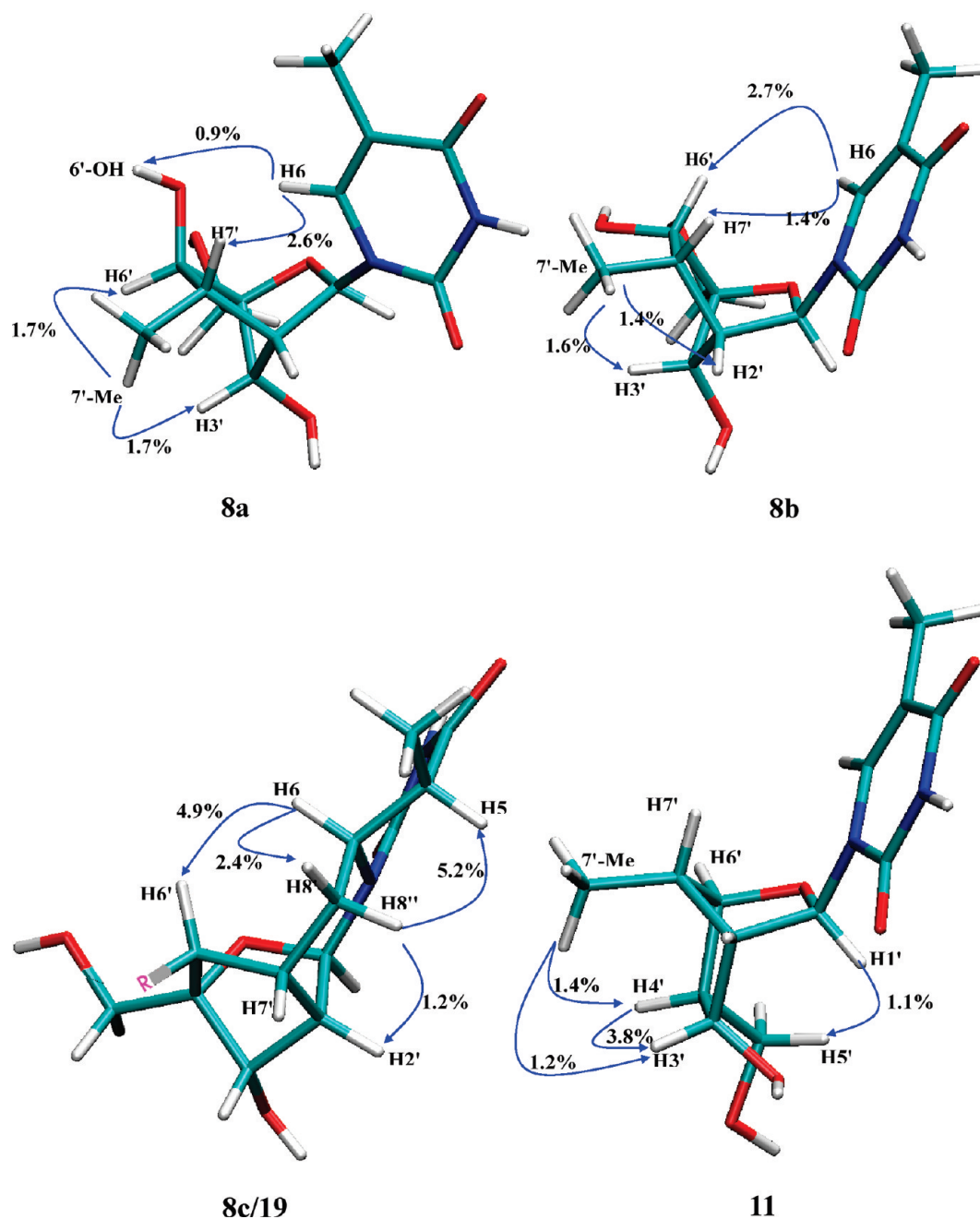(55) Beckwith, A. L. J. *Tetrahedron* **1981**, *37*, 3073−3100.

FIGURE 2. Key NOE contacts of carbocyclic compound **8a**, **8b**, **8c/19**, and **11**; R = OH for **8c**, R = H for **19** (see text for discussions), showing 6′*R* and 7′*S* configuration for compound **8a**, 6′*S* and 7′*S* configuration for compound **8b**, 5*S* and 6*S* configuration for compound **8c/19**, and 3′*R* and 4′*R* configuration for compound **11**.

developing 7′-CH$_2$• radical and 6′-OH are all occupying the axial positions. The steric hindrance between them makes TS2 much more unstable than TS3 because, in the TS3 state the thymine moiety, developing 7′-CH$_2$• radical and 6′-OH are occupying the axial, equatorial, and axial positions, respectively (Scheme 5A). This comparison may explain why the exclusive formation of cyclic product **8a** (6′*R*,7′*S*) has been observed.

Similarly, cyclization of **7b** can proceed through intermediates TS5 and TS6 (Scheme 5B). In TS5, the *cis* orientation of 6′-OH (eq) and 7′-CH$_2$• radical (eq) is unfavored because of steric hindrance, but the orientation between thymine moiety (ax) and 6′-OH (eq) as well as 7′-CH$_2$• radical

(eq) is favored. On the other hand, in TS4, the *trans* orientation of 6′-OH (eq) and 7′-CH$_2$• radical (ax) is favored, but 1,3-diaxial dispostion of thymine (ax) and 7′-CH$_2$• radical (ax) is unfavored. Taking together, cyclization of **7b** through both TS5 and TS6 is possible to give product **8b** and **8c** with TS5 predominating since the products **8b** and **8c** were obtained in a ratio of 3:1. The formation of minor product **8c** starting from TS6 can be easily understood as follows: First, in TS6, the primary −CH$_2$• is not stable and will be intramolecularly trapped by the double bond of the thymine moiety before being quenched by Bu$_3$SnH to give intermediate TS7. Then, the newly formed radical center at C5 of the

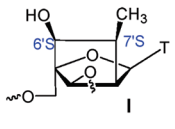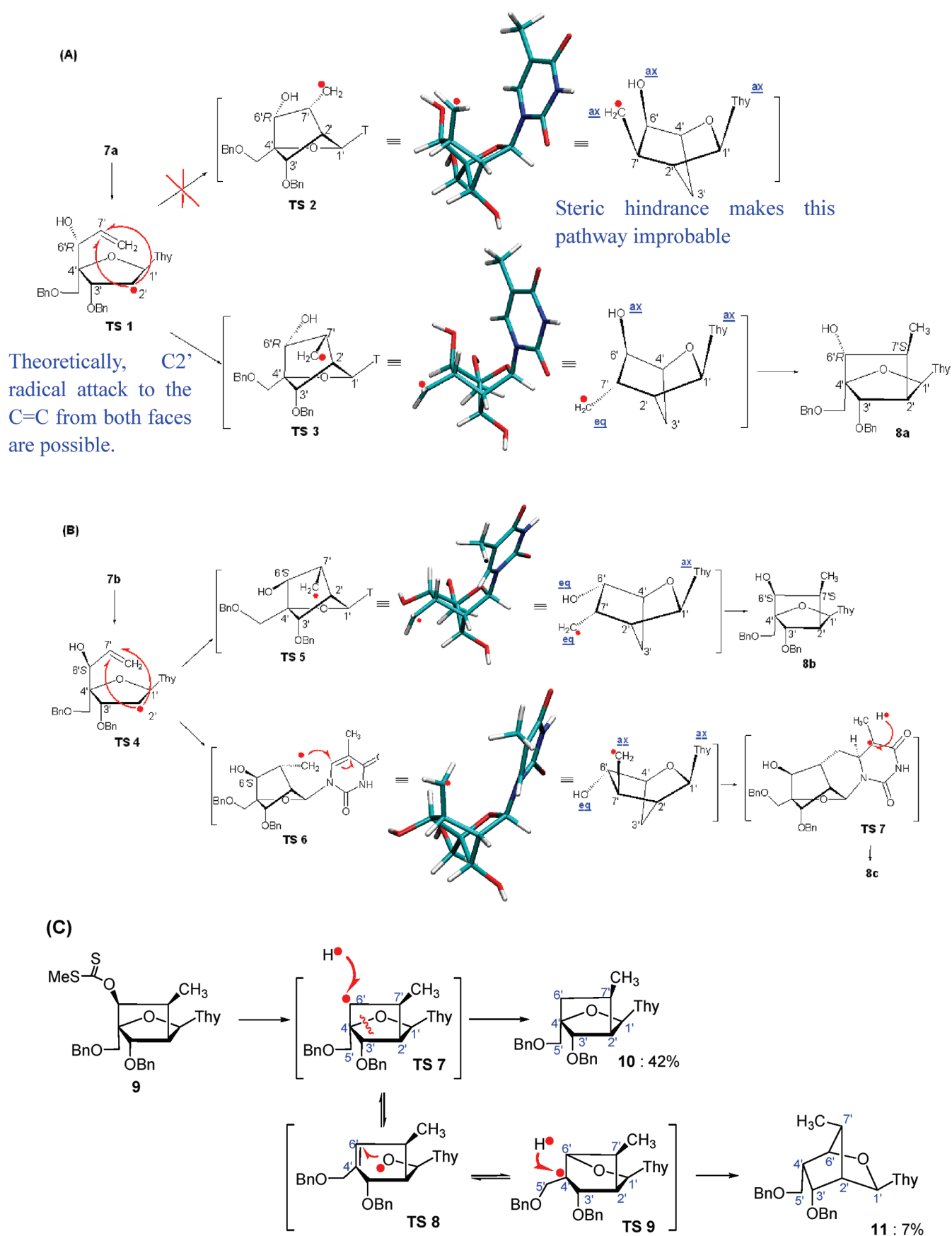**SCHEME 5.** Mechanism of the Formation of 8a, 8b, 8c, and 11 by Intramolecular Free-Radical Cyclization or Rearrangement

Steric hindrance makes this pathway improbable

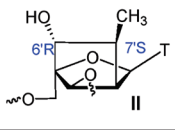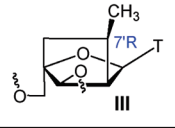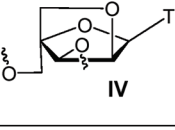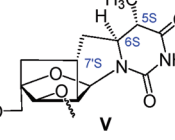Theoretically, C2' radical attack to the C=C from both faces are possible.

TABLE 1. Thermal Denaturation of Duplexes of Native, α-L-Carba-LNA Derivatives and α-L-LNA-Modified AONs with Complementary RNA or DNA[a]

Entry	Modified LNA structures	AON-Sequence* (*Containing modifications in the major groove*)	With RNA $\Delta T_m{}^b$	Major groove Average $\Delta T_m(\text{aver})^b$	With DNA $\Delta T_m{}^b$	Major groove Average $\Delta T_m(\text{aver})^b$	RNA target selectivity $\Delta\Delta T_m{}^c$
AON1	Native	5'-d (CTT CAT TTT TTC TTC)	0[d]		0[d]		
AON2	I	5'-d (CTT CAT TTT TTC *T*TC)	-2.8		-2.6		
AON3		5'-d (CTT CAT TTT *T*TC TTC)	-3.0	-2.9	-5.6	-4.5	+1.6
AON4		5'-d (CTT CAT T*T*T TTC TTC)	-2.2		-5.7		
AON5		5'-d (CTT CA*T* TTT TTC TTC)	-3.6		-4.1		
AON6	II	5'-d (CTT CAT TTT TTC *T*TC)	-2.6		-2.9		
AON7		5'-d (CTT CAT TTT *T*TC TTC)	-2.8	-3.1	-4.5	-4.8	+1.7
AON8		5'-d (CTT CAT T*T*T TTC TTC)	-2.5		-7.0		
AON9		5'-d (CTT CA*T* TTT TTC TTC)	-3.7		-4.6		
AON10	III	5'-d (CTT CAT TTT TTC *T*TC)	-3.0		-4.0		
AON11		5'-d (CTT CAT TTT *T*TC TTC)	-3.0	-3.0	-6.2	-5.6	+2.6
AON12		5'-d (CTT CAT T*T*T TTC TTC)	-2.3		-7.2		
AON13		5'-d (CTT CA*T* TTT TTC TTC)	-3.6		-5.0		
AON14	IV	5'-d (CTT CAT TTT TTC *T*TC)	+3.4		+1.3		
AON15		5'-d (CTT CAT TTT *T*TC TTC)	+5.0	+4.4	+1.8	+1.6	+2.8
AON16		5'-d (CTT CAT T*T*T TTC TTC)	+5.5		+0.9		
AON17		5'-d (CTT CA*T* TTT TTC TTC)	+3.8		+2.2		
AON18	V	5'-d (CTT CAT TTT TTC *T*TC)	-7.6		-6.9		
AON19		5'-d (CTT CAT TTT *T*TC TTC)	-12.6	-12.0	-16.3	-14.4	+2.4
AON20		5'-d (CTT CAT T*T*T TTC TTC)	-13.8		-18.2		
AON21		5'-d (CTT CA*T* TTT TTC TTC)	-13.9		-16.2		

[a]Molecular weights of all antisense sequences are conformed by MALDI-TOF mass spectrum (see Table SII. 2 in Supporting Information). A = native adeninyl, C = cytosinyl, T = thyminyl, '*T*' indicates α-L-carba-LNA or α-L-LNA-modified thymidime monomer with specified structure. T_m values measured as the maximum of the first derivative of the melting curve (A_{260nm} vs T) in medium salt buffer (60 mM Tris-HCl at pH 7.5, 60 mM KCl, 0.8 mM $MgCl_2$) with temperature range of 20 to 65 °C using 1 μM concentrations of the two complementary strands. The value of T_m given is the average of two or three independent measurements. If the error of the first two measurements exceeded ±0.3 °C, the third measurement was carried out to confirm if the error is indeed within ±0.3 °C. [b]ΔT_m values were obtained by comparing the T_m values of AONs **2−21** with that of native AON **1**. The ΔT_m(ave) value obtained here is the average value for four AONs incorporated with the same compound at four different modification sites. [c]The RNA selectivity $\Delta\Delta T_m$ was calculated by this equation: $\Delta\Delta T_m = \Delta T_m(\text{ave})$ of AON/RNA − $\Delta T_m(\text{ave})$ of AON/DNA. [d]T_m of AON1/RNA and AON1/DNA are adopted for T_m comparison; therefore, their ΔT_m values are set to 0.

thymine moiety was reduced by Bu₃SnH from the less sterically hindered face, giving chiral C5 in S-configuration. Hence, tetracyclic nucleoside **8c** was obtained through a radical cyclization process, which is different from that of formation of tetracyclic 2'-amino-α-L-LNA[39] because the latter was obtained through aza-Michael addition of the 2'-amino to C6 position of thymine. Moreover, the formed 2'N−C6 bond in the latter was not stable, and decomposition under basic conditions was observed. Instead, the carbocyclic compound **8c** was found to be a much more stable tetracyclic nucleoside.

In our previous study, a radical deoxygenation of C6'−OH of β-D-carba-LNA led to an unusual 2',6'-methylene-bridged hexopyranosyl nucleoside,[49] which was obtained through a radical rearrangement of the generated 6'C• to 4'C• radicals. The formation of compound **11** during radical deoxygenation of the 6'-OH of α-L-carba-LNA nucleoside **9** was supposed to have gone through a similar mechanism. Thus after treatment of compound **9** with Bu₃SnH and AIBN in refluxing toluene, 6'C• was putatively formed (Scheme 5C), which can be reduced by Bu₃SnH directly to give product **10**. On the other hand, the 6'C• could also lead to scission of the C4'−O4' bond to

give a new C6'=C4' double bond. As a result, the 4'C• radical was transformed to 4'O• (TS8). Then the 4'O• radical attacked the C6'=C4' again, resulting in formation of O4'−C6' bond and the rearrangement of 4'O• radical to 4'C•, which was reacted with Bu₃SnH by the less hindered face to furnish hexopyranosyl nucleoside **11**.

4. Synthesis and Purification of α-L-Carba-LNA Derivatives and α-L-LNA-Modified AONs. The phosphoramidites **16a/b/c** and **22** as well as α-L-LNA monomer[35,36] were incorporated as monosubstitutions, but at four different sites in a 15-mer DNA sequence on an automated RNA/DNA synthesizer. With exception of specially designed fast deprotecting DNA monomer blocks, the standard DNA synthesis reagents and cycles were utilized to synthesize the DNA oligos targeted to coding region of SV 40 large T antigen.[56,57] The sequences, modification site, and structures of modifications are shown in Table 1. All of the modified building blocks gave modest

(56) Graessmann, M.; Michaels, G.; Berg, B.; Graessmann, A. *Nucleic Acids Res.* **1991**, *19*, 53–59.
(57) Wagner, R. W.; Matteucci, M. D.; Lewis, J. G.; Gutierrez, A. J.; Moulds, C.; Froehler, B. C. *Science* **1993**, *260*, 1510–1513.

total coupling yield (20 to 45%). The reduction of coupling yield probably originates from close proximity of the carbocyclic or heterocyclic ring fused on the upper face of the sugar moiety as well as the 6′ and 7′ substituents to the 3′-phosphate, thereby interfering with the coupling and reducing coupling efficiency to some extent. Cleavage from the solid phase support and deprotection steps were carried out by treating the solid support with 33% aqueous ammonia at rt for 12 h (for AONs **10−21**) or at 55 °C for 72 h (deprotection of Tol group used for protection 6′-OH in AONs **2−9** needs a longer deprotection time), followed by purification through 20% denatured PAGE, and confirmation of structural integrity using MALDI-TOF mass spectroscopy (see Table SII.3 in Supporting Information).

5. Thermal Denaturation Studies. The T_m values of duplexes formed by AONs **2−21** with the complementary RNA or DNA have been measured and compared with that of the native counterpart (Table 1). Just as in previous reports,[33−36] one α-L-LNA (type IV) modification resulted in roughly 4.4 °C increase in T_m for the AON/RNA hybrid. On the contrary, 7′*R*-Me-α-L-carba-LNA (type III) led to T_m decrease around 3 °C/modification. Type I and type II modifications, just like the type III modification, also led to T_m decrease by around 3 °C/modification. This observation indicates that 6′-OH in 6′*S*-OH-7′*R*-Me-α-L-carba-LNA (type I) and 6′*R*-OH-7′*R*-Me-α-L-carba-LNA (type II) exert no obvious effect on T_m for the AON/RNA hybrid regardless of their chirality. Hence, the drop in T_m caused by types I, II, and III modification could be due to steric clash of the hydrophobic 7′*R*-methyl group, which points toward vicinal 3′-phosphate ($d_{(7′S\text{-methyl})\text{-}3′P} \approx 4.1$ Å), thereby impairing the AON/RNA thermal stability by perturbing the hydration pattern[58−63] and other stereoelectronic interations in the major groove of the DNA/RNA duplex. Similarly declined T_m results were also observed in the 2′-*N*-ethyl and acetyl functionalized 2′-amino-α-L-LNA-modified AONs, which showed 3−10 °C decrease (sequence dependent) in the thermal stability toward complementary RNA,[40] once again suggesting that the introduction of a bulky hydrophobic group in position pointing at 3′-phosphate in the major groove of the AON/RNA hybrid can cause substantial negative effects on the duplexes' stability.

It is noteworthy that the 6′,7′-substituted β-D-carba-LNA derivatives were found in our previous studies[27−29] to lead to increased T_m by 2−4 °C depending on different substitutions at 6′ and 7′ positions. This should be compared to the observation made in the present study showing a T_m drop of 2−3 °C for 6′,7′-substituted α-L-carba-LNA. This significant difference in thermal stabilities of β-D-carba-LNA vis-à-vis α-L-carba-LNA-modified duplexes hints that the substitutions on the carbocyclic ring of α-L-carba-LNA located in the major groove of DNA/RNA duplex have significantly destabilized the duplex, while the modifications of the carbocyclic ring of β-D-carba-LNA

located in the minor groove lead to stabilization of the duplexes. We have also found that all the α-L-LNA and α-L-carba-LNA derivatives are RNA selective since $\Delta\Delta T_m$ ($\Delta\Delta T_m = \Delta T_m$(ave) of AON/RNA − ΔT_m(ave) of AON/DNA) values were found in the range of 1.6−2.8 °C (Table 1).

Incorporation of the hyperconstrained 6,7′-methylene-bridged-α-L-carba-LNA thymidine (type V) into 15-mer oligonucleotides led to dramatic decrease in thermal affinity toward both complementary RNA and DNA (T_m dropped 7−14 °C with RNA, and dropped 7−18 °C with DNA; see AON **18−21** in Table 1). This result was quite similar to the previous observations that AONs modified by 5*S*,6*R*-configured tetracyclic "locked LNA" also exhibit very low affinity toward complementary RNA and DNA.[39] It was speculated that the loss of aromaticity in nucleobase resulted in the increased steric bulk of the nucleobase moiety (from planar to tetrahedral geometry at C5 and C6 position), thereby destabilizing the duplex owing to perturbation of the base stacking of modified nucleic acid with neighboring base pair to some extent due to energetically unfavorable intrastrand interaction. Alternatively, as a consequence of constrained glycosidic torsion angle of type V, the nucleobase participating in hydrogen bonding might not be disposed optimally for efficient Watson−Crick base pairing, therefore, also impairing the duplexes stability to some extent.

6. Circular Dichroism Analysis. 6.1. CD of AON−RNA Duplex: CD spectra were recorded to evaluate the overall conformation of single modified AON/DNA and AON/RNA duplexes compared to the native DNA/DNA, RNA/RNA, and DNA/RNA duplexes (see Figure 3). As shown in Figure 3A, all of the single modified AON/RNA hybrids exhibited CD profiles intermediate between the native A-type RNA/RNA and B-type DNA/DNA duplexes, but resemble the natural AON **1**/RNA hybrid, which suggested that the single modification with types I, II, III, IV, and V in AONs **4/8/12/16/20** did not cause much conformational perturbation for AON/RNA duplex compared to natural AON **1**/RNA duplex. Hence, types I, II, III, IV, and V modified AON/RNAs could be good substrates for RNase H digestion. Especially, we found that the hyperconstrained tetracyclic 6,7′-methylene-bridged α-L-carba-LNA-Thy (type V) modification led to less conformational perturbation for AON/RNA hybrid than type I, II, III, and IV modifications. As discussed in section 5, the conformationally constrained glycosidic torsion angle of type V modification could however impair its ability to form efficient Watson−Crick base pair with adenine in the opposite strand, thus this type V modified AON strand might perturb the driving force for conformation change necessary in the modified AON strand for forming thermodynamically stable duplex with the target opposite RNA strand.

6.2. CD of AON−DNA Duplex: The duplexes of AONs **4/8/12/16** with complementary DNA also showed relatively similar global helical conformation to the native DNA/DNA homoduplex (shown in Figure 3B). However, the CD profile for the duplex of type V modified AON **20** with complementary DNA was found to obviously shift to shorter wavelength (blue shift) with more intense positive Cotton peak around 276 nm compared with the native AON **1**/DNA duplex. Hence, it seems a single type V modification can significantly perturb the global conformation of AON/DNA duplex.

(58) Teplova, M.; Minasov, G.; Teresshko, V.; Inamati, G. B.; Cook, P. D.; Manoharan, M.; Egli, M. *Nat. Struct. Biol.* **1999**, *6*, 535−539.

(59) Egli, M.; Minasov, G.; Teplova, M.; Kumar, R.; Wengel, J. *Chem. Commun.* **2001**, 651−652.

(60) Schneider, B.; Patel, K.; Berman, H. M. *Biophys. J.* **1998**, *75*, 2422−2434.

(61) Tereshko, V.; Gryaznov, S.; Egli, M. *J. Am. Chem. Soc.* **1998**, *120*, 269−283.

(62) Auffinger, P.; Westhof, E. *Angew. Chem., Int. Ed.* **2001**, *40*, 4648−4650.

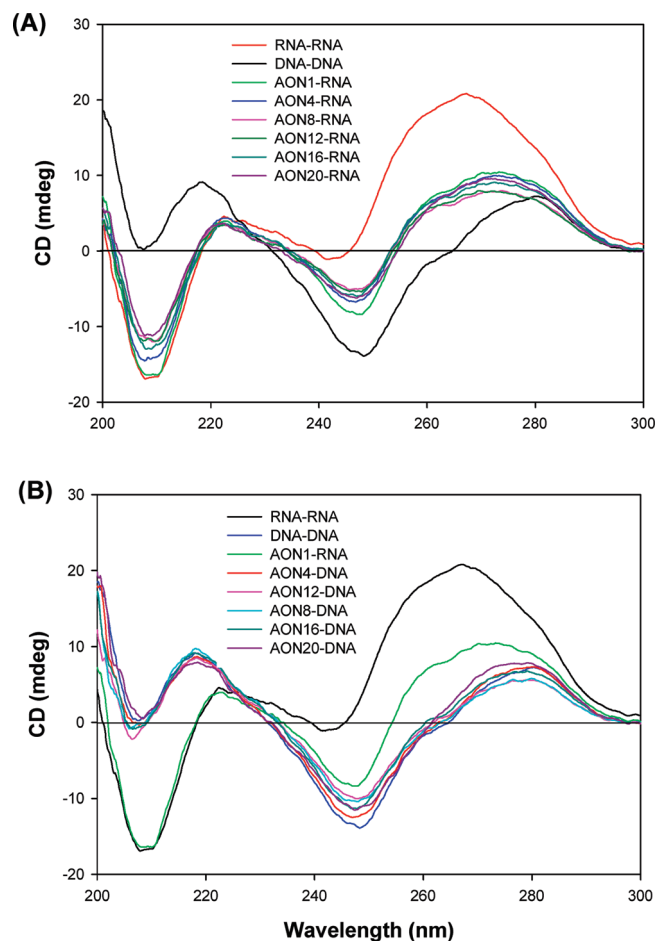(63) Ball, P. *Chem. Rev.* **2008**, *108*, 74−108.

FIGURE 3. CD spectra of duplexes formed by AON **1/4/8/12/16/20** with complementary RNA (A) or DNA (B). Typical B-type (DNA/DNA duplex) and A-type (RNA/RNA duplex) spectra are also presented for comparison. Native DNA/DNA duplex was formed by the native AON **1** with complementary DNA, while native RNA/RNA duplex was formed by 3′-r(CUU CUU UUU UAC UUC) with complementary RNA. The CD spectra were measured in the same buffer as used for UV melting experiment (Table 1) at 20 °C. The total strand concentration is 10 μM.

7. Comparison of 3′-Exonuclease Stabilities of AONs Containing α-L-Carba-LNA Derivatives with the Parent α-L-LNA. It is known that 3′-exonuclease activity is predominantly responsible for enzymatic degradation of AON in serum-containing medium or in various eukaryotic cell lines, and modifications located at 3′-terminus can significantly contribute to the nuclease resistance of an oligonucleotide.[64] The stabilities of the newly synthesized AONs (AON **2**, **6**, **10**, **14**, **18**) with a single modification (types I, II, III, IV, V) at position T13 (position 3 from 3′-end) toward 3′-exonuclease (phosphodiesterase I from *Crotalus adamateas* venom [SVPDE] used in this study) were measured. Thus the selected AONs were labeled at the 5′-end with ^{32}P-ATP/kinase and then incubated with SVPDE [SVPDE 6.7 ng/μL, AON 3 μM, 100 mM Tris-HCl (pH 8.0), 15 mM MgCl$_2$, total volume 30 μL] at 21 °C. Aliquots were taken out at appropriate time intervals and analyzed by 20% denaturing PAGE. The gel pictures were obtained upon autoradiography and are shown in Figure SII.44 in Supporting Information.

(64) Maier, M. A.; Leeds, J. M.; Balow, G.; Springer, R. H.; Bharadwaj, R.; Manoharan, M. *Biochemistry* **2002**, *41*, 1323–1327.

The native AON was completely degraded in ∼10 min under present conditions. All of the other modified AONs containing α-L-carba-LNA derivatives showed considerably improved 3′-exonuclease resistance to a variable extent. Because the AONs were singly modified at position T13, the phosphate P14 (see the structure in Figure 4A for phosphate (P) numbering) was considerably resistant to 3′-exonuclease cleavage. Moreover, T13 modification also improves the stability of P13 phosphate to some extent. Therefore, two bands referring to 14-mer and 13-mer oligos could be observed on the PAGE pictures (Figure SII.44). However, once the P13 was cleaved, AONs were degraded to the monomer blocks quickly, and hence no bands referring to 12-mer to dimer oligos could be observed.

Total percentages of intergrated 14-mer and 13-mer AONs were plotted against time points to give SVPDE digestion curve for each selected AON in Figure 4B, and pseudo-first-order reaction rates (Figure 4B and Table SII.2) were obtained by fitting the curves to single-exponential decay functions. A comparison of digestion rates of AONs with different types of modifications exhibited the following results and implications:

7.1. Relative 3′-Exonucleolytic Stabilities of α-L-Carba-LNA-Modified AONs. The stabilities of AONs **2**, **6**, **10**, **14**, **18** toward SVPDE incubation decreased in following order: 6,7′-methylene-bridged α-L-carba-LNA-T (type V) modified AON **18** ($k = 0.0040 \pm 0.0012$ min^{-1}) > 7′R-methyl-α-L-carba-LNA (type III) modified AON **10** ($k = 0.0068 \pm 0.0009$ min^{-1}) ≈ 6′R-hydroxyl-7′S-methyl-α-L-carba-LNA (type II) modified AON **6** ($k = 0.0076 \pm 0.0018$ min^{-1}) > 6′S-hydroxyl-7′S-methyl-α-L-carba-LNA (type I) modified AON **2** ($k = 0.0125 \pm 0.0007$ min^{-1}) > α-L-LNA (type IV) modified AON **14** ($k = 0.0777 \pm 0.0072$ min^{-1}) > β-D-LNA (type VI) incorporated AON ($k = 0.5331 \pm 0.1800$ min^{-1}). Hence, all α-L-carba-LNA analogue modified AONs have been found to be 3′-exonucleolytically more stable than parent α-L-LNA and β-D-LNA-modified counterparts. Another strategy, namely, phosphorothioate backbone modification, is also popular to produce AONs with high nucleolytic stability, but this type of modification, on the other hand, can lead to extensive cellular toxicity and side effects.[1] Hence, α-L-carba-LNA-modified AONs with phosphodiester linkage probably will show better pharmacologic properties than AONs containing both α-L (or β-D)-LNA and phosphorothioate backbone modifications.

7.2. Effect of 7′-Me Substitution on 3′-Exonucleolytic Stability. We have found that 7′R-methyl-α-L-carba-LNA (type III) modified AON **10** is about 10 times more stable than α-L-LNA (type IV) modified AON **14**, which suggests that the replacement of the 2′-*O*- with hydrophobic methyl-methylene function in α-L-LNA can render significantly positive effects on the nuclease resistance.

7.3. Effect of 6′R-OH Substitution (Pointing away from 3′-Phosphate) on 3′-Exonucleolytic Stability. C6′−OH substitution on the α-L-carba-LNA can modulate the stability of modified AONs to different extent depending on the stereochemical orientation of the hydroxyl group. 6′R-Hydroxyl substitution led to virtually no effect since 6′R-hydroxyl-7′S-methyl-α-L-carba-LNA (type II) modified AON **6** have shown very similar overall stability with the 7′R-methyl-α-L-carba-LNA (type III) modified AON **10**. We have also found the 6′R-OH substitution can improve the nuclease resistance for the vicinal 5′-phosphate as can be seen from the
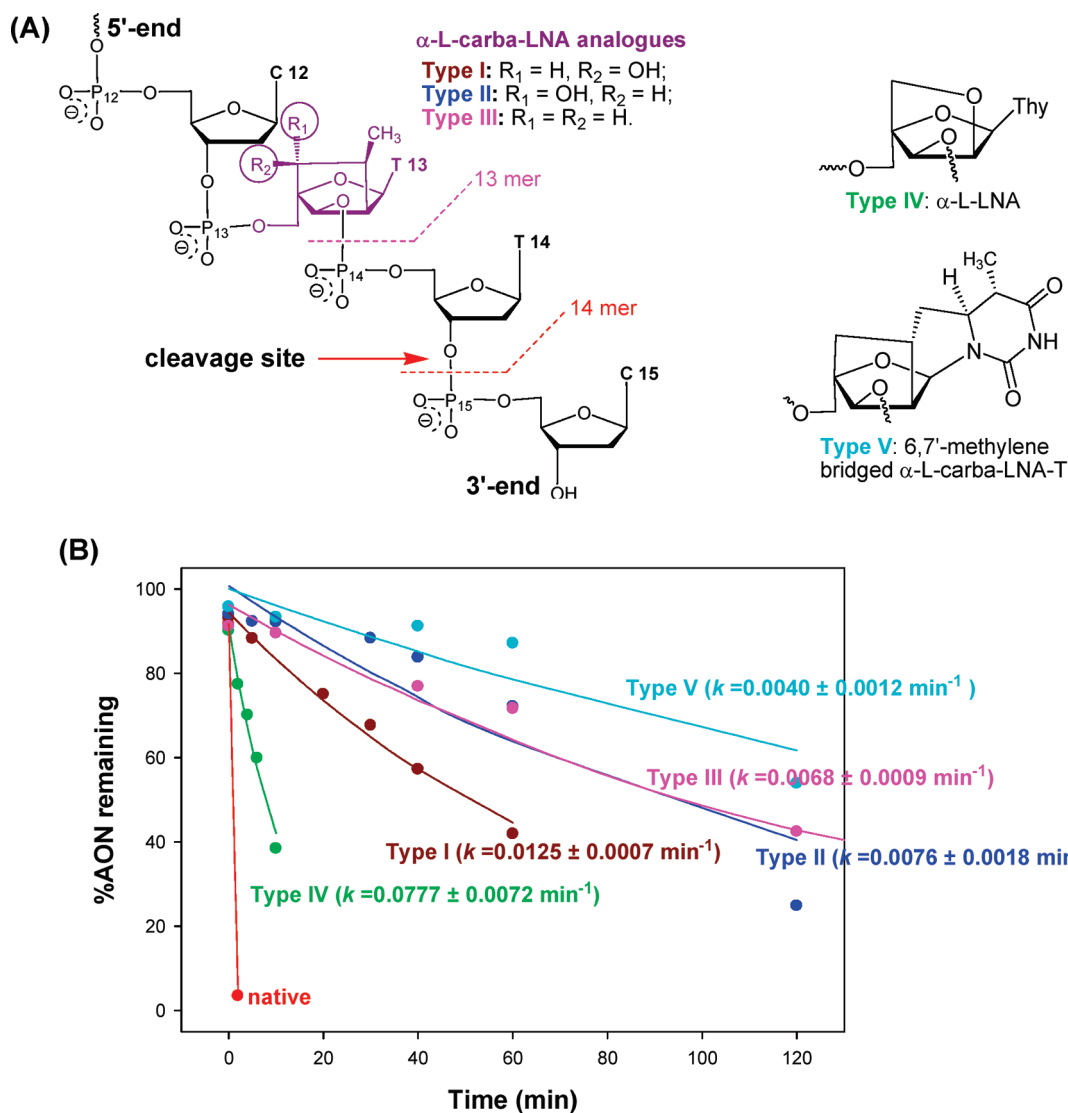
FIGURE 4. (A) Molecular structure of T13 modified AONs. The full sequence is 3′-d (CT$\underline{T}$[13]CTT TTT TAC TTC-^{32}P)-5′. (B) Amount of remaining initial oligonucleotide (taken 14-mer and 13-mer together in the calculation of percentage remaining) during 3′-exonuclease (SVPDE) promoted digestion. The digestion conditions were used as follows: AON 3 μM (5′-end ^{32}P-labeled with specific activity 80 000 cpm), 100 mM Tris-HCl (pH 8.0), 15 mM MgCl$_2$, SVPDE 6.7 ng/μL, reaction temperature 21 °C, total reaction volume 30 μL.

band corresponding to 13-mer oligo which was observed in PAGE for type II modified AON **6** while the 13-mer band was not present for type I modified AON **2** and type III modified AON **10** (Figure SII.44 in Supporting Information). Effectively the 6′R-OH protects the 5′-phosphate by interfering with binding of SVPDE to this phosphate.[32] Indeed the 6′R-OH in 6′R-hydroxyl-7′S-methyl-α-L-carba-LNA (type II) has been found located relatively close to the 5′-phosphate ($d_{5′R\text{-OH-}5′P} \approx 4.0$ Å).

7.4. Effect of 6′S-OH Substitution (Pointing at 3′-Phosphate) on 3′-Exonucleolytic Stability. Previous study[32] has shown that in β-D-carba-LNA 6′-OH substitution can remarkably reduce 3′-exonucleolytic stability of modified AONs if this OH points at the vicinal 3′-phosphate probably because of its assistance in the departure of 3′-oxyanion during SVPDE mediated 3′O−P bond scission.[32] Similar conclusions can be reached in the present investigation as 6′S-hydroxyl substitution [OH group is also pointing at the vicinal 3′-phosphate] in 6′S-hydroxyl-7′S-methyl-α-L-carba-LNA (type I) leads,

upon incorporation into modified AON **2**, to significantly less 3′-exonucleolytic stable duplex than the duplex incorporating the 7′R-methyl-α-L-carba-LNA (type III) modification (AON **10**).

7.5. Effect of Tetracyclic System on 3′-Exonucleolytic Stability. 6,7′-Methylene-bridged α-L-carba-LNA-T (type V) modified AON **18** showed better 3′-exonucleolytic resistance than type I, II, and III modified AONs. It can be concluded that the extra six-membered ring of 6,7′-methylene-bridged α-L-carba-LNA-T (type V), which lies above the pentose sugar, gave slightly higher nuclease resistance compared to other α-L-carba-LNA derivatives (types I, II, and III).

Comparison of 3′-exonucleolytic resistance of α-L-carba-LNA-modified AONs with that of β-D-LNA and β-D-carba-LNA-modified counterparts has also been carried out. Corresponding PAGE, 3′-exonuclease (SVPDE) promoted digestion plot and discussion can be found in part II of Supporting Information.

8. Relationship between 3′-Exonuclease Stability and Solvation Free Energy for α-L-Carba-LNA Derivatives and Parent α-L-LNA. The solvation properties of modified AON affect the relative access of the water molecule to the scissile phosphate, therefore giving variable extent of 3′-exonuclease resistance. In order to check the relationship between solvation capability and nuclease stability of AONs with different modifications, we have analyzed the solvation free energy of α-L-carba-LNA derivatives (types I, II, III) as well as that of the parent α-L-LNA (type IV) (Table SII.1) employing Baron and Cossi's implementation of polarizable conductor CPCM model[65] of solvation on the *ab initio* optimized (HF,6-31G** basis set) gas phase molecular geometries. The solvation free energies obtained have clearly demonstrated relative hydrophilic nature of different 2′,4′-constrained modifications in α-L-carba-LNA and α-L-LNA. The energy of solvation of α-L-carba-LNA derivatives (types I, II, III) and α-L-LNA (type IV) decreases in the following order: 7′R-methyl-α-L-carba-LNA (type III, -3.04 kcal mol^{-1}) > 6′R-hydroxyl-7′S-methyl-α-L-carba-LNA (type II, -4.30 kcal mol^{-1}) > 6′S-hydroxyl-7′S-methyl-α-L-carba-LNA (type I, -4.35 kcal mol^{-1}) > α-L-LNA (type IV, -8.51 kcal mol^{-1}). This trend shows the α-L-carba-LNA derivatives are not as well solvated as the parent α-L-LNA, which suggests the scissile phosphate of α-L-LNA is relatively more solvated as compared to that of α-L-carba-LNA derivatives. The magnitudes of 3′-exonuclease stability of these α-L-2′,4′-constrained nucleoside modified AONs have also shown the following decreasing trend: 7′R-methyl-α-L-carba-LNA (type III, $k = 0.0068 \pm 0.0009$ min^{-1}) ≈ 6′R-hydroxyl-7′S-methyl-α-L-carba-LNA (type II, $k = 0.0076 \pm 0.0018$ min^{-1}) > 6′S-hydroxyl-7′S-methyl-α-L-carba-LNA (type I, $k = 0.0125 \pm 0.0007$ min^{-1}) ≫ α-L-LNA (type IV, $k = 0.0777 \pm 0.0072$ min^{-1}), which is fully consistent with the results from solvation free energy calculation. This corroborated our original hypothesis that the hydration around a scissile phosphate was most probably critical for the nuclease-promoted hydrolysis.[27]

9. Stability of Functionalized α-L-Carba-LNA-Modified AONs in Human Blood Serum. The newly synthesized AONs with a single modification types I, II, III, IV, and V at position T13 (position 3 from 3′-end) were assayed for stability in human blood serum. The AONs (5′-end ^{32}P-labeled) were incubated with human blood serum (male, type AB) for up to 48 h at 21 °C, and aliquots were taken out at regular time intervals and then analyzed by 20% denaturing PAGE. The gel pictures obtained by autoradiography are shown in Figure SII.43. Due to the presence of alkaline phosphatase in blood serum that gradually removes the 5′-end ^{32}P label, it was impossible to obtain accurate degradation rate for each AON by quantifying the gel picture. Visual comparison of the gel pictures have shown that 6′S-hydroxyl-7′S-methyl-α-L-carba-LNA (type I) modified AON **2** and 7′R-methyl-α-L-carba-LNA (type III) modified AON **10** can be sustained in blood serum for more than 48 h. These modifications result in more stable AONs compared to 6′R-hydroxyl-7′S-methyl-α-L-carba-LNA (type II) modified AON **6** and 6,7′-methylene-bridged α-L-carba-LNA-T (type V) modified AON **18**, which is sustained for 36 h in blood serum. The α-L-LNA (type IV) modified AON

14 exhibited the least stability in human blood serum. The order of relative stabilities of AONs in human blood serum has been found to be similar to that observed upon treatment by 3′-exonucleases.

10. RNase H Digestion Studies of Functionalized α-L-Carba-LNA-Modified AON/RNA Duplexes. It has been reported that RNase H binds in the minor groove of the DNA/RNA hybrid.[66,67] Hence α-L-carba-LNA modifications are supposed to have relatively minor effect on the RNase H recruitment than β-D-carba-LNA modification because the 2′,4′-carbocyclic ring in the former is located in the major groove but the carbocyclic ring in the latter is located in the minor groove of the AON/RNA hybrid. Hence, the RNase H recruitment study of four newly synthesized α-L-carba-LNA derivative modified AONs (containing a single type I, II, III, or V modification) as well as the parent α-L-LNA-modified AON (type IV) has been carried out and compared with the native AON **1** as well as with the β-D-carba-LNA-modified AONs.[27−29]

The gel pictures in Figure SII.37−39 have shown that all the modified AONs **2−21**/RNA hybrids are good substrates for RNase H. For type I, II, III, and IV modified AON/RNA duplexes, the cleavage patterns have been found to be very similar and independent of the nature of the modification but dependent on the site of modification. As shown in Figure 5A, the cleavage activity of RNase H was suppressed within a stretch of a 5 base pairs region that starts from the modification site toward the 3′-end in the RNA strand. In addition, the original preferred A8 cleavage site also shifted to the edges of suppressed region if A8 is included within this 5 bp suppressed area. Hence, the observed RNase H cleavage patterns for type I, II, III, and IV modified AON/RNA duplexes were found to be very closely similar to the previous studies of β-D-carba-LNA,[27−29] β-D-carba-ENA,[27,28] and β-D-aza-ENA[20,21] modified AON/RNA hybrids, suggesting that RNase H does not make any distinction on whether the 2′,4′-carbocylcic ring is located in the minor or the major groove, it renders very similar cleavage pattern.

However, it is interesting to note that tetracyclic 6,7′-methylene-bridged α-L-carba-LNA (type V) modified AON **19**/RNA and AON **20**/RNA hybrids showed different cleavage patterns compared to the type I, II, III, and IV modified AON/RNA duplexes at the same position: a stretch of 3 bp region was observed for RNase H cleavage suppression in AON **19**/RNA duplex, whereas a stretch of 5 bp suppressed region was also observed in AON **20**/RNA duplex but with different preferred cleavage site and suppressed stretch region (see Figure 5B). This result hints that type V modification led to relatively less conformational perturbation for AON/RNA hybrid than type I, II, III, and IV modifications, which is consistent with the result obtained by CD study.

All the α-L-carba-LNA derivative modified AON/RNA duplexes were degraded by RNase H with comparable cleavage rates as digestion of native AON/RNA hybrid (Figure 6). Remarkably, the cleavage rates of types III (7′R-methyl-α-L-carba-LNA) and IV (α-L-LNA) modified AON/RNA duplex were even 2 times higher than cleavage of

(65) Barone, V.; Cossi, M. *J. Phys. Chem. A* **1998**, *102*, 1995–2001.

(66) Nowotny, M.; Gaidamakov, S. A.; Crouch, R. J.; Yang, W. *Cell* **2005**, *121*, 1005–1016.

(67) Nowotny, M.; Cerritelli, S. M.; Ghirlando, R.; Gaidamakov, S. A.; Crouch, R. J.; Yang, W. *EMBO J.* **2008**, *27*, 1172–1181.

(A)

AON 1 (Native DNA)

AON 3/7/11/15

AON 2/6/10/14/18

AON 4/8/12/16

AONs 5/9/13/17/21

(B)

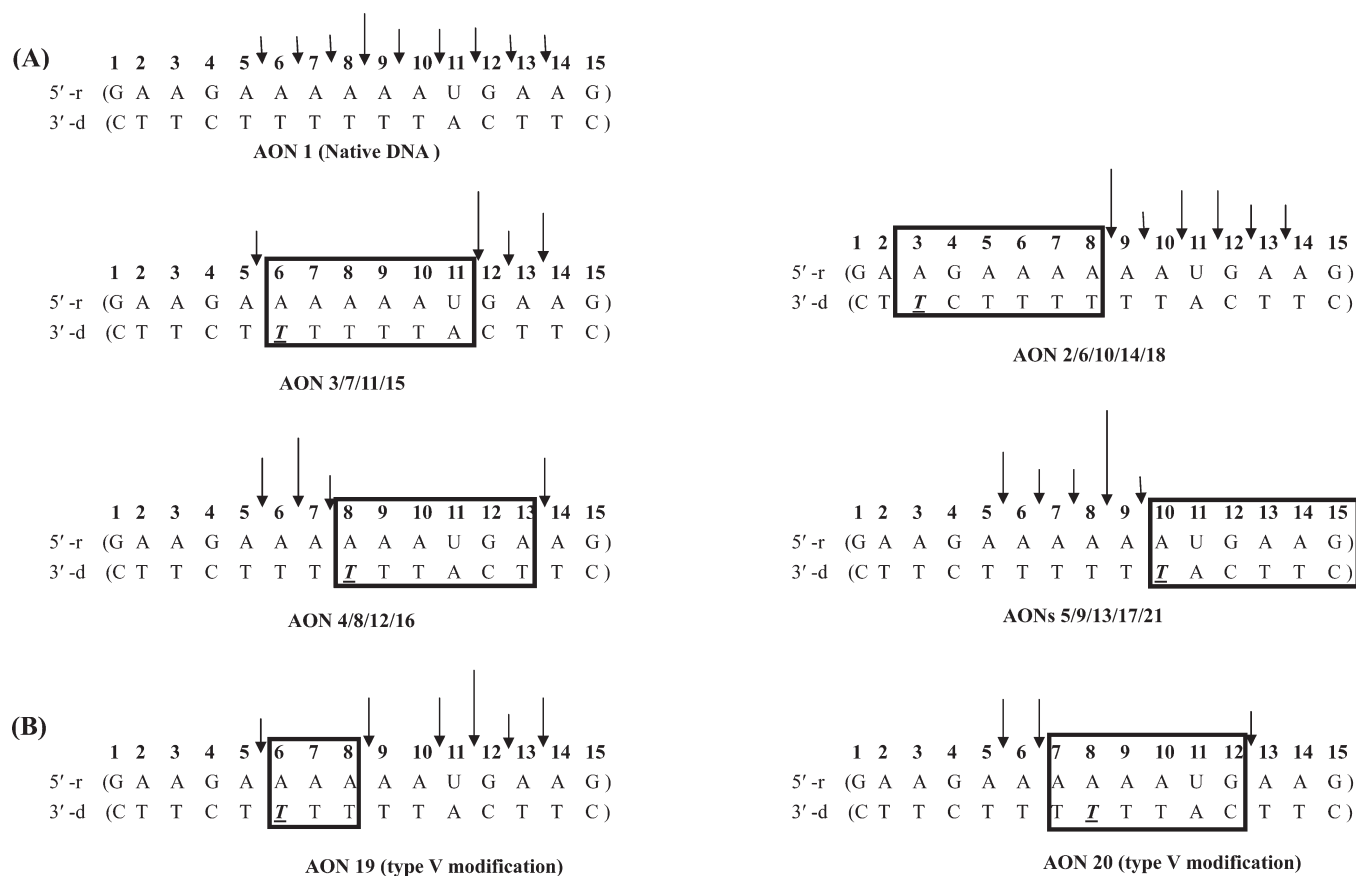**AON 19 (type V modification)**

AON 20 (type V modification)

FIGURE 5. *Escherichia coli* RNase H1 promoted cleavage pattern of AONs **1−21**/RNA heteroduplexes. Vertical arrows show the RNase H cleavage sites, with the relative length of the arrow indicating the extent of the cleavage. The square boxes show the stretch of the modification, which is resistant to RNase H1 cleavage, thereby giving footprints.

the native counterpart. Given that β-D-carba-LNA-modified AON/RNA duplexes generally showed less RNase H digestion efficiency than the native counterpart,[28,29] we could arrive at the conclusion that α-L-carba-LNA modifications led to much less effect on RNase H elicitation than β-D-carba-LNA modification. This is because of the fact that the stereochemical location of the hydrophobic 2′,4′-carbocyclic ring in β-D-carba-LNA is in the minor groove, which retards the RNase H binding in the minor groove, but, in contrast, that is not the case for the α-L-carba-LNA since its 2′,4′-carbocyclic ring is located in the major groove.

Conclusion

1. Herein, we report convenient synthetic routes toward the α-L-carba-LNA thymidine derivatives. The synthesis of these novel α-L-*ribo*-configured conformationally constrained carbocyclic analogues has been achieved by employing free-radical scavenging by a tethered olefin in an intramolecular reaction as a key step. Various NMR experiments, including ^{1}H, ^{13}C, ^{1}H−^{1}H COSY, one-bond ^{1}H−^{13}C correlation (HMQC), and long-range ^{1}H−^{13}C HMBC have been carried out to characterize all synthesized compounds unambiguously. The relative chirality of substituents in the key intermediates was determined by 1D NOE and was also corroborated by the $^{3}J_{HH}$ coupling constants obtained from H−H homo or double decoupling experiments.

2. The thermal denaturation study of duplexes formed by AON containing a single α-L-carba-LNA derivatives with complementary RNA revealed that T_{m} of 6′,7′-substituted α-L-carba-LNA-modified AON/RNA is about 3 °C lower than that of the native AON/RNA and 7 °C lower than that of the parent α-L-LNA-modified counterpart. This suggests that the hydration perturbation in the major groove caused by the substitution of α-L-carba-LNA results in more negative effects on duplex thermal stability compared to the substitution of β-D-carba-LNA derivatives in minor groove.

3. Substituted α-L-carba-LNA-modified AONs have been found in presence of both snake venom phosphodiesterase and human blood serum to be more stable than the parent α-L-LNA and β-D-LNA-modified counterparts.

4. α-L-Carba-LNA derivatives and α-L-LNA-modified AON/RNA duplexes have shown similar RNase H digestion pattern as the β-D-carba-LNA-modified counterparts, but better digestion efficiency. Especially, the cleavage rates of types III (7′*R*-methyl-α-L-carba-LNA) and IV (α-L-LNA) modified AON/RNA duplex were, in some sequences, even 2 times faster than cleavage rates of the native counterpart, suggesting the α-L-carba-LNA modification in which the 2′,4′-carbocyclic ring is located in the major groove can lead to a positive effect on the RNase H digestion efficiency of AON/RNA.
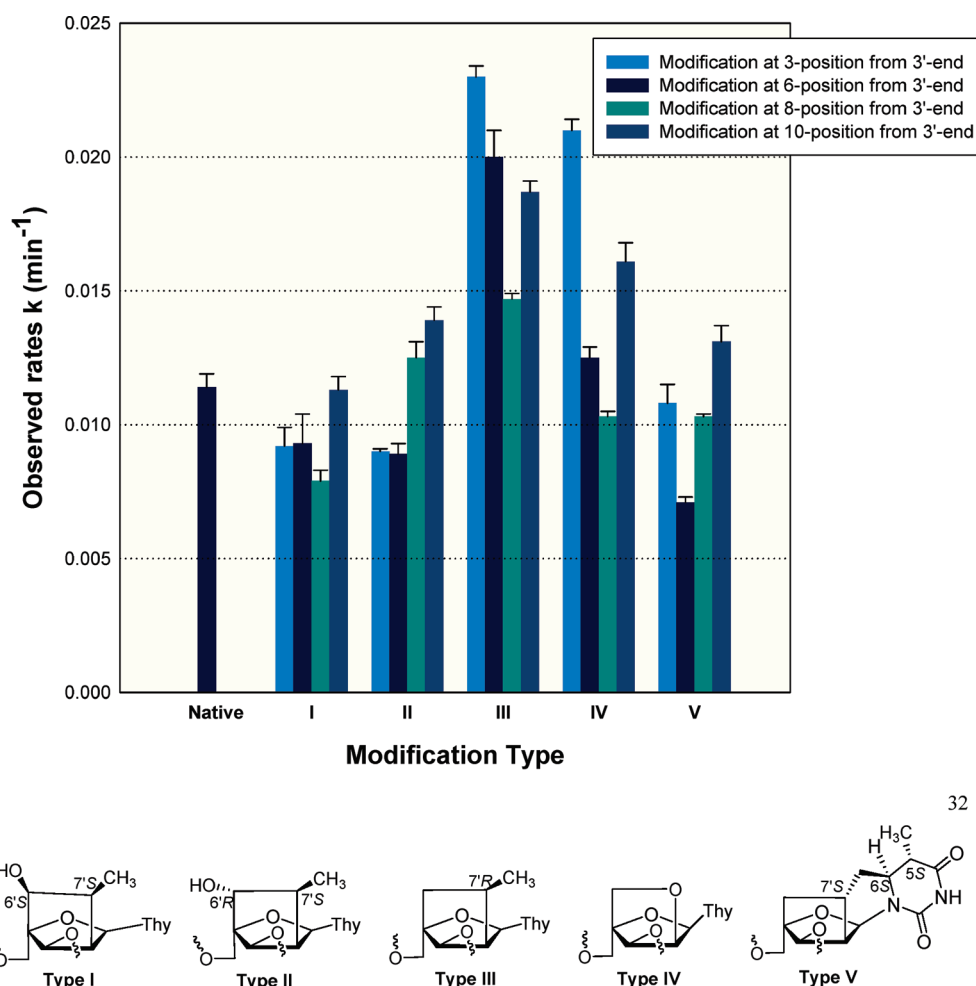
FIGURE 6. Bar plots of the observed cleavage rates of the RNase H1 promoted degradation of RNA in AON **1−21**/RNA hybrid duplexes.

Implication. The obvious merit of introduction of α-L-carba-LNA derivatives into AONs is that they can improve nuclease resistance while rendering positive effect on the RNase H digestion. Unfortunately, all four newly synthesized α-L-carba-LNA derivatives in the present study led to lower RNA affinity (around −3 °C/modification compared to native counterpart). As discussed in section 5, the decrease in the RNA affinity probably originates from the steric clash with the hydrophobic 7′R-methyl group in α-L-carba-LNA, which points toward vicinal 3′-phosphate, thereby impairing the AON/RNA thermal stability by perturbing the hydration pattern in the major groove of the DNA/RNA duplex. Work is in progress to replace 7′R-methyl group with less steric and less hydrophobic hydrogen atom as in parent α-L-carba-LNA [structure (O) in Figure 1] which upon introduction into AONs should hopefully lead to a more effective antisense therapeutic candidate, thereby will further add to the value of α-L-carba-LNA as a modified nucleoside in the AON or siRNA. We anticipate that this parent α-L-carba-LNA should have (1) higher target RNA affinity, just like α-L-LNA, (2) significantly increased enzymatic stability compared to α-L-LNA, and (3) better RNase H elicitation efficiency than α-L-LNA, β-D-LNA, and β-D-carba-LNA derivatives.

Experimental Section

3,5-Di-*O*-benzyl-4-C-(1*R*-hydroxylallyl)-1,2-*O*-isopropylidene-β-L-ribofuranose (3a) and 3,5-Di-*O*-benzyl-4-C-(1*S*-hydroxylallyl)-1,2-

***O*-isopropylidene-β-L-ribofuranose (3b).** Oxalyl chloride (2.84 mL, 32 mmol) was added to the precooled dichloromethane (92 mL) at −78 °C. Then DMSO (3.90 mL, 54 mmol) in dichloromethane (8 mL) was added dropwise to the solution over 30 min. After stirring for 20 min, a solution of **1** (5.20 g, 13.0 mmol) in dichloromethane (24 mL) was added dropwise over about 20 min, and the mixture was kept stirring at −78 °C for another 30 min. DIPEA (16 mL) was added to this cooled mixture. The reaction solution was then allowed to warm to room temperature and stirred for 1 h whereupon water (10 mL) was added. The organic layer was separated, washed with water (50 mL) and brine (50 mL), dried over MgSO$_4$, and concentrated under reduced pressure to give the corresponding aldehyde 2 as a yellowish oil. This oil was dissolved in THF (130 mL) under nitrogen and cooled to 0 °C. Vinyl magnesium bromide (1.0 M solution in THF, 26 mL, 26 mmol) was added, and then the reaction was allowed to warm to room temprature and kept stirring at this temperature overnight. The reaction was slowly quenched with saturated ammonia chloride solution (10 mL). Then the mixture was partitioned between ethyl acetate (150 mL) and water (100 mL), the organic layer was then washed with saturated NaHCO$_3$ and brine, dried over MgSO$_4$, and concentrated under reduced pressure. The crude material was purified by column chromatography on silica gel (0−20% ethyl acetate in cyclohexane, v/v) to give **3a** (1.80 g, 32%) and **3b** (1.61 g, 29%) as colorless oil. **3a**: ^{1}H NMR (500 MHz, CDCl$_3$ + DABCO) δ 7.3−7.2 (10H, m, Bn), 5.73 (1H, m, H7), 5.69 (1H, d, $J_{H1, H2}$ = 3.5 Hz, H1), 5.28 (1H, d, J = 17.5 Hz, H8), 5.13 (1H, d, J = 10.5 Hz, H8′), 4.60 (1H, d, J_{gem} = 11.5 Hz, CH$_2$Bn), 4.57 (1H, d, J_{gem} = 11.5 Hz, CH$_2$Bn), 4.53 (1H, d,

J_{gem} = 11.5 Hz, C$\underline{H_2}$Bn), 4.52 (1H, d, J_{gem} = 11.5 Hz, C$\underline{H_2}$Bn), 4.48 (1H, m, H6), 4.45 (1H, m, H2), 4.05 (1H, d, $J_{H2, H3}$ = 5.0 Hz, H3), 3.99 (1H, d, J_{gem} = 11.0 Hz, H5), 3.74 (1H, d, J_{gem} = 11.0 Hz, H5′), 2.74 (s, DABCO), 1.43 (3H, s, C$\underline{H_3}$), 1.23 (3H, s, C$\underline{H_3}$); ^{13}C NMR (125 MHz, CDCl$_3$ + DABCO) δ 137.2 (Bn), 136.6 (Bn), 133.7 (C7), 127.3−126.5 (aromatic), 116.0 (C8), 112.4 (isopropyl), 103.3 (C1), 87.7 (C4), 77.8 (C2), 76.3 (C3), 72.6 (C6), 71.6 (C$\underline{H_2}$Bn), 71.3 (C$\underline{H_2}$Bn), 69.2 (C5), 45.9 (DABCO), 25.7 (C$\underline{H_3}$), 25.1 (C$\underline{H_3}$); MALDI-TOF m/z [M + Na]$^+$, found 449.199, calcd 449.194. **3b**: ^{1}H NMR (500 MHz, CDCl$_3$) δ 7.3−7.2 (10H, m, Bn), 5.84 (1H, m, H7), 5.59 (1H, d, $J_{H1, H2}$ = 3.0 Hz, H1), 5.31 (1H, d, J = 17.5 Hz, H8), 5.15 (1H, d, J = 11.0 Hz, H8′), 4.68 (1H, d, J_{gem} = 12.0 Hz, C$\underline{H_2}$Bn), 4.56 (1H, d, J_{gem} = 12.0 Hz, C$\underline{H_2}$Bn), 4.53 (1H, d, J_{gem} = 12.0 Hz, C$\underline{H_2}$Bn), 4.52 (1H, d, J_{gem} = 12.0 Hz, C$\underline{H_2}$Bn), 4.46 (1H, t, H2), 4.35 (1H, m, H6), 4.06 (1H, d, J_{gem} = 10.5 MHz, H5), 3.99 (1H, d, $J_{H2, H3}$ = 5.5 Hz, H3), 3.81 (1H, d, J_{gem} = 10.5 MHz, H5′), 2.79 (1H, d, J = 6.0 Hz 6-OH), 1.45 (3H, s, C$\underline{H_3}$), 1.25 (3H, s, C$\underline{H_3}$); ^{13}C NMR (125 MHz, CDCl$_3$) δ 136.9 (Bn), 136.7 (Bn), 135.0 (C7), 127.3−126.6 (aromatic), 115.9 (C8), 112.6 (isopropyl), 103.0 (C1), 86.1 (C4), 78.7 (C2), 76.3 (C3), 73.8 (C6), 72.8 (C$\underline{H_2}$Bn), 71.4 (C$\underline{H_2}$Bn), 70.4 (C5), 25.9 (C$\underline{H_3}$), 25.3 (C$\underline{H_3}$); MALDI-TOF m/z [M + Na]$^+$, found 449.198, calcd 449.194.

1-[4-C-(1R-Acetoxyallyl)-2,6-di-O-acetyl-3,5-di-O-benzyl-α-L-ribofuranosyl]thymine (5a). Acetic anhydride (2.44 mL, 25 mmol) and acetic acid (85 mL) were added to **3a** (1.80 g, 4.2 mmol). The mixture was cooled with ice bath, and triflic acid (0.02 mL, 0.14 mmol) was added. After stirring for 2 h at room temperature, the reaction was quenched with cold saturated NaHCO$_3$ solution (20 mL) and extracted with dichloromethane (50 mL × 3), the organic layer was separated, dried over MgSO$_4$, and evaporated to dryness to furnish crude product **4a**, which was coevaporated with anhydrous CH$_3$CN twice and dissolved in the same solvent. Thymine (720 mg, 5.70 mmol) and N,O-bis(trimethylsilyl)acetamide (2.9 mL, 11.8 mmol) were added to the solution and refluxed for 45 min until the suspension became a clear solution. Then reaction mixture was cooled to 0 °C, and TMSOTf (1.1 mL, 6.10 mmol) was added dropwise, then the reaction was refluxed overnight. CH$_3$CN was evaporated under reduced pressure. To the residue was added saturated ammonia chloride solution (10 mL), and the mixture was extracted with dichloromethane (50 mL). The organic layer was dried over MgSO$_4$, evaporated, and chromatographed over silica gel (0−1% methanol in dichloromethane, v/v) to give **5a** as a white foam (1.84 g, 76%): ^{1}H NMR (600 MHz, CDCl$_3$ + DABCO) δ 7.3−7.1 (Bn), 6.95 (1H, s, H6), 6.00 (1H, d, $J_{H1′, H2′}$ = 5.4 Hz, H1′), 5.70 (1H, d, $J_{H6′, H7′}$ = 4.8 Hz, H6′), 5.62 (1H, m, H7′), 5.26 (1H, d, J = 16.8 Hz, H8′), 5.16 (1H, m, H2′), 5.16 (1H, d, J = 10.8 Hz, H8′′), 4.55 (1H, d, J_{gem} = 12.6 Hz, C$\underline{H_2}$Bn), 4.44 (1H, d, J_{gem} = 12.6 Hz, C$\underline{H_2}$Bn), 4.43 (1H, d, J_{gem} = 12.6 Hz, C$\underline{H_2}$Bn), 4.34 (1H, d, J_{gem} = 12.6 Hz, C$\underline{H_2}$Bn), 4.32 (1H, m, H3′), 3.69 (1H, d, J_{gem} = 10.8 Hz, H5′), 3.50 (1H, d, J_{gem} = 10.8 Hz, H5′′), 2.79 (s, DABCO), 2.06 (3H, s, acetyl-C$\underline{H_3}$), 1.94 (3H, s, acetyl-C$\underline{H_3}$), 1.82 (3H, s, 5-C$\underline{H_3}$); ^{13}C NMR (150 MHz, CDCl$_3$ + DABCO) δ 169.3 (C=O, acetyl), 167.9 (C=O, acetyl), 162.8 (C4), 149.5 (C2), 136.5 (aromatic), 135.9 (aromatic), 134.3 (C6), 130.4 (C7′), 127.5−126.8 (aromatic), 118.3 (C8′), 110.5 (C5), 86.8 (C4′), 85.3 (C1′), 74.9 (C3′), 73.5 (C6′), 73.4 (C$\underline{H_2}$Bn), 72.8 (C2′), 72.7 (C$\underline{H_2}$Bn), 67.9 (C5′), 45.4 (DABCO), 20.2 (acetyl-C$\underline{H_3}$), 19.6 (acetyl-C$\underline{H_3}$), 11.6 (5-C$\underline{H_3}$); MALDI-TOF m/z [M + Na]$^+$, found 601.217, calcd 601.216.

1-[3,5-Di-O-benzyl-2,6-dihydroxyl-4-C-(1R-hydroxylallyl)-α-L-ribofuranosyl]thymine (6a). Compound **5a** (1.0 g, 1.70 mmol) was treated with 30% methylamine solution in ethanol (60 mL) at room temperature overnight. Then the reaction mixture was evaporated to dryness and purified by column chromatography on silica gel (0−3% methanol in dichloromethane, v/v) to give **6a** (872 mg, 100%) as a white solid: ^{1}H NMR (500 MHz, CDCl$_3$)

δ 7.3−7.2 (Bn), 7.03 (1H, s, H6), 5.69 (1H, m, H7′), 5.36 (1H, d, J = 16.5 Hz, H8′), 5.34 (1H, d, $J_{H1′, H2′}$ = 5.4 Hz, H1′), 5.15 (1H, d, J = 10.5 Hz, H8′′), 4.61 (1H, d, J_{gem} = 11.0 Hz, C$\underline{H_2}$Bn), 4.49 (1H, m, H2′), 4.49 (1H, d, J_{gem} = 11.0 Hz, C$\underline{H_2}$Bn), 4.46 (1H, m, H3′), 4.42 (1H, d, J_{gem} = 11.0 Hz, C$\underline{H_2}$Bn), 4.41 (1H, d, J_{gem} = 11.0 Hz, C$\underline{H_2}$Bn), 4.24 (1H, d, $J_{H6′, H7′}$ = 5.5 Hz, H6′), 3.77 (1H, d, J_{gem} = 10.0 Hz, H5′), 3.76 (1H, s, 2′−OH), 3.42 (1H, s, 6′−OH), 3.37 (1H, d, J_{gem} = 10.0 Hz, H5′′), 1.83 (3H, s, 5-C$\underline{H_3}$); ^{13}C NMR (125 MHz, CDCl$_3$) δ 162.5 (C4), 149.6 (C2), 138.6 (C6), 136.4 (aromatic), 135.8 (aromatic), 133.8 (C7′), 127.6−126.9 (aromatic), 116.9 (C8′), 110.0 (C5), 97.4 (C1′), 89.2 (C4′), 74.2 (C3′), 73.2 (C6′), 72.8 (C$\underline{H_2}$Bn), 72.1 (C$\underline{H_2}$Bn), 71.9 (C2′), 70.6 (C5′), 11.2 (5-C$\underline{H_3}$); MALDI-TOF m/z [M + Na]$^+$, found 517.200, calcd 517.195.

1-[3,5-Di-O-benzyl-4-C-(1R-hydroxylallyl)-6-hydroxyl-2-O-phenoxythiocarbonyl-α-L-ribofuranosyl]thymine (7a). Compound **6a** (872 mg, 1.70 mmol) was coevaporated twice with anhydrous pyridine and dissolved in the same solvent (38 mL). The solution was cooled by ice bath, and then phenyl chlorothionoformate (0.29 mL, 2.10 mmol) was added dropwise, while temperature was maintained at 0 °C during addition. After 3 h of stirring at room temperature, pyridine was recovered under reduced pressure. The residue was dissolved in dichloromethane (50 mL) and washed with saturated solution of NaHCO$_3$ (20 mL). The organic layer was separated, dried over MgSO$_4$, and concentrated in vacuo. Crude product was chromatographed over silica gel (10−25% ethyl acetate in cyclohexane, v/v) to afford **7a** (920 mg, 86%) as a white foam: ^{1}H NMR (500 MHz, CDCl$_3$) δ 8.61 (1H, br s, N$\underline{H}$), 7.30−7.17 (13H, m, aromatic), 6.86 (2H, d, J = 8.0 Hz, aromatic), 5.94 (1H, app t, H2′), 5.81 (1H, d, $J_{H1′, H2′}$ = 6.0 Hz, H1′), 5.70 (1H, m, H7′), 5.46 (1H, d, J = 17.0 Hz, H8′), 5.17 (1H, d, J = 10.5 Hz, H8′′), 4.63 (1H, d, $J_{H2′, H3′}$ = 6.5 Hz, H3′), 4.59 (1H, d, $J_{H6′, H7′}$ = 5.5 Hz, H6′), 4.56 (1H, d, J_{gem} = 12.0 Hz, C$\underline{H_2}$Bn), 4.55 (1H, d, J_{gem} = 12.0 Hz, C$\underline{H_2}$Bn), 4.45 (1H, d, J_{gem} = 12.0 Hz, C$\underline{H_2}$Bn), 4.44 (1H, d, J_{gem} = 12.0 Hz, C$\underline{H_2}$Bn), 3.73 (1H, d, J_{gem} = 11.0 Hz, H5′), 3.52 (1H, d, J_{gem} = 11.0 Hz, H5′′), 3.29 (1H, bs, 6′−OH), 1.85 (3H, s, 5-C$\underline{H_3}$); ^{13}C NMR (125 MHz, CDCl$_3$) δ 193.2 (C=S), 152.3 (C4), 149.4 (C2), 137.5 (C6), 136.6 (aromatic), 136.2 (aromatic), 133.8 (C7′), 128.6−125.8 (aromatic), 120.8 (aromatic), 116.7 (C8′), 110.4 (C5), 89.5 (C4′), 89.3 (C1′), 80.0 (C2′), 73.8 (C3′), 73.7 (C$\underline{H_2}$Bn), 72.9 (C$\underline{H_2}$Bn), 71.9 (C6′), 69.0 (C5′), 11.4 (5-C$\underline{H_3}$); MALDI-TOF m/z [M + Na]$^+$, found 653.197, calcd 653.193.

(1S,3R,4S,5S,6R,7S)-7-Benzyloxy-1-benzyloxymethyl-6-hydroxy-5-methyl-3-(thymin-1-yl)-2-oxabicyclo[2.2.1]heptane (8a). Compound **7a** (974 mg, 1.55 mmol) was dissolved in 140 mL of anhydrous toluene that was purged with N$_2$ for half an hour. The mixture was heated to reflux and Bu$_3$SnH (0.41 mL in 12 mL of anhydrous toluene, 1.55 mmol) and AIBN (293 mg in 24 mL anhydrous toluene, 1.55 mmol) were added dropwise in four portions over 4 h. Then the refluxing was continued for another 1 h. Solvent was evaporated, and the residue was purified by column chromatography on silica gel (20−40% ethyl acetate in cyclohexane, v/v) to give **8a** (420 mg, 57%) as a white solid: ^{1}H NMR (600 MHz, CDCl$_3$) δ 8.63 (1H, br s, N$\underline{H}$), 8.16 (1H, s, H6), 7.30−7.18 (10H, m, Bn), 6.16 (1H, d, $J_{H1′, H2′}$ = 2.4 Hz, H1′), 4.63 (1H, d, J_{gem} = 12.0 Hz, C$\underline{H_2}$Bn), 4.62 (1H, d, J_{gem} = 12.0 Hz, C$\underline{H_2}$Bn), 4.45 (1H, d, J_{gem} = 12.0 Hz, C$\underline{H_2}$Bn), 4.44 (1H, d, J_{gem} = 12.0 Hz, C$\underline{H_2}$Bn), 3.86 (1H, d, $J_{H2′, H3′}$ = 1.5 Hz, H3′), 3.81 (1H, m, H6′), 3.81 (1H, d, J_{gem} = 10.2 Hz, H5′), 3.74 (1H, d, J_{gem} = 10.2 Hz, H5′′), 2.83 (1H, s, 6′−OH), 2.63 (1H, m, H2′), 1.86 (3H, s, 5-C$\underline{H_3}$), 1.56 (1H, m, H7′), 0.95 (3H, d, $J_{7′-CH3, H7′}$ = 7.8 Hz 7′-C$\underline{H_3}$); ^{13}C NMR (125 MHz, CDCl$_3$) δ 163.1 (C4), 149.3 (C2), 137.8 (C6), 136.2 (aromatic), 136.1 (aromatic), 127.6−126.6 (aromatic), 107.6 (C5), 88.6 (C1′), 88.1 (C4′), 80.4 (C3′), 78.9 (C6′), 73.1 (C$\underline{H_2}$Bn), 70.8 (C$\underline{H_2}$Bn), 68.1 (C5′), 47.8 (C2′), 32.3 (C7′), 25.9 (cyclohexane, coming from chromatography elution

solvent), 17.8 (7′-CH$_3$), 11.4 (5-CH$_3$); MALDI-TOF m/z [M + Na]$^+$, found 501.203, calcd 501.200.

(1S,3R,4S,5S,6S,7S)-7-Benzyloxy-1-benzyloxymethyl-6-hydroxyl-5-methyl-3-(thymin-1-yl)-2-oxabicyclo[2.2.1]heptane (8b) and (1R,6S,7S,9R,10S,11S,12S,13S)-12-Benzyloxy-11-benzyloxymethyl-2,4-diaza-10-hydroxyl-6-methyltetracyclo[9,2,1,0^{2,7}0^{9,13}]-tetradecan-3,5-dione (8c). Compound **7b** (3.0 g, 4.76 mmol) was dissolved in 410 mL of anhydrous toluene that was purged with N$_2$ for 30 min prior to use. The mixture was heated to reflux and Bu$_3$SnH (1.26 mL in 44 mL anhydrous toluene, 4.76 mmol) and AIBN (899 mg in 92 mL of anhydrous toluene, 4.76 mmol) were added dropwise in four portions over 4 h. Then the refluxing was continued for another 1 h. Solvent was evaporated, and the residue was purified by column chromatography on silica gel (20−40% ethyl acetate in cyclohexane, v/v, then 0−0.5% methanol in dichloromethane, v/v) to give **8b** (986 mg, 43%) and **8c** (310 mg, 14%) as white solids. **8b**: ^{1}H NMR (500 MHz, CDCl$_3$) δ 8.74 (1H, s, NH), 7.36 (1H, s, H6), 7.30−7.23 (Bn), 5.95 (1H, d, $J_{H1', H2'}$ = 2.5 Hz, H1′), 4.63 (1H, d, J_{gem} = 11.5 Hz, CH$_2$Bn), 4.62 (1H, d, J_{gem} = 11.5 Hz, CH$_2$Bn), 4.48 (1H, d, J_{gem} = 11.5 Hz, CH$_2$Bn), 4.47 (1H, d, J_{gem} = 11.5 Hz, CH$_2$Bn), 4.15 (1H, s, $J_{H2', H3'}$ = 1.5 Hz, H3′), 3.97 (1H, dd, $J_{H6', H7'}$ = 8.5 Hz, $J_{H6', 6'-OH}$ = 3.0 Hz, H6′), 3.90 (1H, d, J_{gem} = 11.0 Hz, H5′), 3.81 (1H, d, J_{gem} = 11.0 Hz, H5″), 2.68 (1H, d, $J_{H6', 6'-OH}$ = 3.0 Hz, 6′-OH), 2.66 (1H, m, H2′), 1.92 (1H, m, H7′), 1.86 (3H, s, 5-CH$_3$), 0.89 (3H, d, $J_{7'-CH3, H7'}$ = 7.5 Hz 7′-CH$_3$); ^{13}C NMR (125 MHz, CDCl$_3$): δ 162.9 (C4), 148.8 (C2), 136.4 (aromatic), 136.3 (aromatic), 134.9 (C6), 127.6−126.7 (aromatic), 108.3 (C5), 88.1 (C4′), 87.9 (C1′), 80.3 (C3′), 72.9 (C6′), 71.3 (CH$_2$Bn), 71.3 (CH$_2$Bn), 66.3 (C5′), 46.3 (C2′), 29.1 (C7′), 25.9 (cyclohexane, coming from chromatography solvent), 11.7 (7′-CH$_3$), 11.4 (5-CH$_3$); MALDI-TOF m/z [M + Na]$^+$, found 501.202, calcd 501.200. **8c**: ^{1}H NMR (500 MHz, CDCl$_3$) δ 7.77 (1H, s, NH), 7.28−7.18 (10H, m, Bn), 6.36 (1H, d, $J_{H1', H2'}$ = 2.0 Hz, H1′), 4.57 (1H, d, J_{gem} = 12.0 Hz, CH$_2$Bn), 4.56 (1H, d, J_{gem} = 12.0 Hz, CH$_2$Bn), 4.49 (1H, d, J_{gem} = 12.0 Hz, CH$_2$Bn), 4.41 (1H, d, J_{gem} = 12.0 Hz, CH$_2$Bn), 4.04 (1H, d, $J_{H2', H3'}$ = 2.0 Hz, H3′), 3.84 (1H, d, J_{gem} = 10.5 Hz, H5′), 3.75 (1H, app t, H6′), 3.74 (1H, d, J_{gem} = 10.5 Hz, H5″), 3.29 (1H, ddd, $J_{H5, H6}$ = 10.5 Hz, $J_{H8', H6}$ = 4.0 Hz, $J_{H8'', H6}$ = 12.0 Hz, H6), 3.09 (1H, d, $J_{H6', 6'-OH}$ = 2.0 Hz, 6′-OH), 2.29 (1H, m, $J_{H5, H6}$ = 10.5 Hz, $J_{H5, 5-CH3}$ = 7.0 Hz, H5), 2.19 (1H, app tt, $J_{H8', H6}$ = 4.0 Hz, $J_{H8', H7'}$ = 3.5 Hz, $J_{H8', H8''}$ = 13.5 Hz, H8′), 2.15 (1H, m, H2′), 1.95 (1H, m, $J_{H8', H7'}$ = 3.5 Hz, $J_{H8'', H7'}$ = 4.0 Hz, $J_{H6', H7'}$ = 2.0 Hz, H7′), 1.35 (1H, m, $J_{H8'', H6}$ = 12.0 Hz, $J_{H8'', H7'}$ = 4.0 Hz, $J_{H8', H8''}$ = 13.5 Hz, H8″), 1.18 (1H, d, $J_{H5, 5-CH3}$ = 7.0 Hz, 5-CH$_3$); ^{13}C NMR (125 MHz, CDCl$_3$) δ 169.6 (C4), 152.7 (C2), 136.8 (aromatic), 136.3 (aromatic), 127.6−126.6 (aromatic), 84.5 (C4′), 81.1 (C3′), 80.3 (C1′), 74.4 (C6′), 72.9 (CH$_2$Bn), 71.3 (CH$_2$Bn), 66.6 (C5′), 47.8 (C6), 40.2 (C5), 39.0 (C2′), 36.2 (C7′), 30.2 (C8′), 9.8 (5-CH$_3$); MALDI-TOF m/z [M + Na]$^+$, found 501.201, calcd 501.200.

(1S,3R,4S,5S,6R,7S)-7-Benzyloxy-1-benzyloxymethyl-5-methyl-6-(4-methylbenzoate)-3-(thymin-1-yl)-2-oxabicyclo[2.2.1]heptane (12a). Compound **8a** (285 mg, 0.60 mmol) was coevaporated with anhydrous pyridine twice and dissolved in the same solvent (10 mL). The mixture was cooled with an ice bath, and 4-methyl benzoyl chloride (0.12 mL, 0.90 mmol) was added dropwise to this precooled solution. The mixture was allowed to stir at room temperature for 6 h. Pyridine was recovered under reduced pressure, and the residue was dissolved in dichloromethane (10 mL). The obtained solution was washed with saturated NaHCO$_3$ aqueous solution (10 mL), dried over MgSO$_4$, and concentrated under reduced pressure to give crude product, which was subjected to short column chromatography on silica gel (15−30% ethyl acetate in cyclohexane, v/v) to afford **12a** (260 mg, 73%): ^{1}H NMR (500 MHz, CDCl$_3$) δ 8.69 (1H, br s, NH), 7.82 (1H, s, H6), 7.80 (2H, m, aromatic), 7.29−7.10 (12H, m, aromatic), 6.06 (1H, d, $J_{H1', H2'}$ = 2.5 Hz, H1′), 4.91 (1H, d, $J_{H6', H7'}$ = 4.0 Hz, H6′), 4.67 (1H, d, J_{gem} = 12.0 Hz, CH$_2$Bn), 4.60 (1H, d, J_{gem} = 12.0 Hz, CH$_2$Bn),

4.49 (1H, d, J_{gem} = 12.0 Hz, CH$_2$Bn), 4.48 (1H, d, J_{gem} = 12.0 Hz, CH$_2$Bn), 4.13 (1H, s, H3′), 3.70 (1H, d, J_{gem} = 9.5 Hz, H5′), 3.62 (1H, d, J_{gem} = 9.5 Hz, H5″), 2.79 (1H, s, H2′), 2.36 (3H, s, Tol-CH$_3$), 1.65 (1H, m, H7′), 1.46 (3H, s, 5-CH$_3$), 1.20 (3H, d, $J_{7'-CH3, H7'}$ = 7.0 Hz 7′-CH$_3$); ^{13}C NMR (125 MHz, CDCl$_3$) δ 164.9 (Tol-C=O), 162.9 (C4), 149.0 (C2), 143.3 (aromatic), 136.5 (aromatic), 136.3 (aromatic), 136.2 (C6), 128.6−125.8 (aromatic), 107.9 (C5), 88.7 (C1′), 88.3 (C4′), 78.9 (C3′), 78.0 (C6′), 72.6 (CH$_2$Bn), 71.1 (CH$_2$Bn), 62.4 (C5′), 48.2 (C2′), 31.9 (C7′), 20.7 (Tol-CH$_3$), 17.4 (7′-CH$_3$), 11.0 (5-CH$_3$); MALDI-TOF m/z [M + H]$^+$, found 597.262, calcd 597.260.

(1S,3R,4S,5S,6R,7S)-1-(4,4′-Dimethoxytrityloxymethyl)-7-hydroxyl-5-methyl-6-(4-methylbenzoate)-3-(thymin-1-yl)-2-oxabicyclo[2.2.1]heptane (13a). To a solution of compound **12a** (252 mg, 0.420 mmol) in anhydrous methanol (10 mL) were added 20% Pd(OH)$_2$/C (315 mg) and ammonium formate (1.60 g, 25.5 mmol), and the mixture was refluxed for 2 h. The suspension was filtered over Celite, and the organic phase was evaporated in vacuo to give crude **12a′**, which was coevaporated twice with anhydrous pyridine and dissolved in the same solvent (6 mL). 4,4′-Dimethoxytrityl chloride (282 mg, 0.84 mmol) was added, and the mixture was stirred overnight at room temperature. Then solvent was removed, and the residue was diluted with dichloromethane (10 mL), washed with aqueous saturated NaHCO$_3$ solution (10 mL), and dried over MgSO$_4$. After evaporation of solvent, the residue was subjected to column chromatography on silica gel (0.3−1.2% methanol in dichloromethane containing 1% pyridine, v/v) to afford **13a** (225 mg, 75%): ^{1}H NMR (500 MHz, CDCl$_3$ + DABCO) δ 7.73 (1H, s, H6), 7.71 (2H, m, aromatic), 7.33−7.08 (11H, m, aromatic), 6.68 (4H, m, aromatic), 6.14 (1H, d, $J_{H1', H2'}$ = 2.5 Hz, H1′), 4.89 (1H, d, $J_{H6', H7'}$ = 4.0 Hz, H6′), 4.47 (1H, d, $J_{H2', H3'}$ = 1.0 Hz, H3′), 3.62 (3H, s, CH$_3$O), 3.59 (3H, s, CH$_3$O), 3.48 (1H, d, J_{gem} = 10.0 Hz, H5′), 3.37 (1H, d, J_{gem} = 10.0 Hz, H5″), 2.76 (s, DABCO), 2.72 (1H, s, H2′), 2.36 (3H, s, Tol-CH$_3$), 1.63 (1H, m, H7′), 1.41 (1H, s, 5-CH$_3$), 1.26 (3H, d, $J_{7'-CH3, H7'}$ = 7.5 Hz 7′-CH$_3$); ^{13}C NMR (125 MHz, CDCl$_3$ + DABCO) δ 164.9 (Tol-C=O), 163.2 (C4), 157.5 (aromatic), 149.4 (C2), 143.4 (aromatic), 136.1 (C6), 134.5 (aromatic), 134.1 (aromatic), 129.0−124.3 (aromatic), 112.2 (aromatic), 107.9 (C5), 88.8 (C1′), 85.7 (C4′), 79.0 (OCPh$_3$), 78.9 (C6′), 73.3 (C3′), 56.9 (C5′), 54.1 (CH$_3$O), 50.8 (C2′), 45.7 (DABCO), 32.1 (C7′), 20.7 (Tol-CH$_3$), 17.6 (7′-CH$_3$), 10.9 (5-CH$_3$); MALDI-TOF m/z [M + Na]$^+$, found 741.283, calcd 741.279.

(1S,3R,4S,5S,6R,7R)-1-(4,4′-Dimethoxytrityloxymethyl)-7-hydroxyl-5-methyl-6-(4-methylbenzoate)-3-(thymin-1-yl)-2-oxabicyclo[2.2.1]heptane (15a). Compound **13a** (115 mg, 0.160 mmol) was dissolved in anhydrous dichloromethane (4 mL), and 15% Dess−Martin periodinane in CH$_2$Cl$_2$ (0.67 mL, 0.320 mmol) was added dropwise under nitrogen. After stirring at room temperature for 3 h, the reaction was quenched by aqueous saturated Na$_2$S$_2$O$_3$ (1 mL) and NaHCO$_3$ solution (1 mL), extracted with dichloromethane (10 mL × 3). The organic layer was then dried over MgSO$_4$ and concentrated to dryness to give **14a**. The obtained crude product **14a** was dissolved in 95% ethanol (3 mL), and NaBH$_4$ (12 mg, 0.320 mmol) was added in portions. The mixture was allowed to stir at room temperature for 1 h. Then the solvent was removed, and the residue was extracted with dichloromethane. The organic layer was washed with aqueous saturated NaHCO$_3$ solution, dried over MgSO$_4$, and concentrated under reduced pressure. The residue obtained was subjected to short column chromatography on silica gel (0.3−1.2% methanol in dichloromethane containing 1% pyridine, v/v) to furnish **15a** (66 mg, 57%): ^{1}H NMR (500 MHz, CDCl$_3$ + DABCO) δ 7.78 (2H, m, aromatic), 7.72 (1H, s, H6), 7.34−7.09 (11H, m, aromatic), 6.71 (4H, m, aromatic), 5.84 (1H, d, $J_{H1', H2'}$ = 2.5 Hz, H1′), 5.25 (1H, d, $J_{H6', H7'}$ = 4.0 Hz, H6′), 4.49 (1H, s, H3′), 3.66 (3H, s, CH$_3$O), 3.64 (3H, s, CH$_3$O), 3.49

(2H, dd, J_{gem} = 10.5 Hz, 10.5 Hz, H5′, 5″), 2.75 (s, DABCO), 2.68 (1H, s, H2′), 2.36 (3H, s, Tol-C$\underline{H}_3$), 1.77 (1H, m, H7′), 1.51 (1H, s, 5-C$\underline{H}_3$), 1.39 (3H, d, $J_{7′\text{-CH3, H7}′}$ = 7.0 Hz 7′-C$\underline{H}_3$); ¹³C NMR (125 MHz, CDCl₃ + DABCO) δ 165.1 (Tol-$\underline{C}$=O), 163.2 (C4), 157.6 (aromatic), 149.5 (C2), 143.3 (aromatic), 135.5 (C6), 134.3 (aromatic), 134.2 (aromatic), 129.0−124.3 (aromatic), 112.2 (aromatic), 108.0 (C5), 87.7 (C4′), 86.2 (C1′), 85.8 (O$\underline{C}$Ph₃), 81.7 (C6′), 77.2 (C3′), 58.9 (C5′), 54.1 ($\underline{C}$H₃O), 48.9 (C2′), 45.6 (DABCO), 34.3 (C7′), 20.7 (Tol-$\underline{C}$H₃), 17.4 (7′-$\underline{C}$H₃), 11.0 (5-$\underline{C}$H₃); MALDI-TOF m/z [M + Na]⁺, found 741.281, calcd 741.279.

(1S,3R,4S,5S,6S,7S)-7-Benzyloxy-1-benzyloxymethyl-5-methyl-6-((methylthio)thiocarbonyl)oxy-3-(thymin-1-yl)-2-oxabicyclo[2.2.1]-heptane (9). To a solution of compound **8b** (190 mg, 0.40 mmol) in dry THF (6 mL) was added 60% NaH (48 mg, 1.19 mmol) at 0 °C, After stirring at rt for 1 h, CS₂ (0.24 mL, 3.97 mmol) was added to the suspension at 0 °C, and the resulting mixture was added to stirred at rt for another 1 h. The solution became clear and was cooled by ice. Methyl iodide (0.16 mL, 2.60 mmol) was added at 0 °C, and the mixture was stirred at rt for 2 h. The reaction was quenched by chilled water (2 mL) and extracted with ethyl acetate (10 mL) three times. The organic layer was dried over MgSO₄ and evaporated to dryness. The residue was chromatographed over silica gel (15−35% ethyl acetate in cyclohexane) to give compound **9** (145 mg, 64%): ¹H NMR (600 MHz, CDCl₃) δ 8.77 (1H, s, N$\underline{H}$), 7.52 (1H, s, H6), 7.38−7.28 (10H, m, aromatic), 6.10 (1H, d, $J_{\text{H1}′, \text{H2}′}$ = 1.8 Hz, H1′), 5.89 (1H, d, $J_{\text{H6}′,\text{H7}′}$ = 8.4 Hz, H6′), 4.74 (1H, d, J_{gem} = 11.4 Hz, C$\underline{H}_2$Bn), 4.69 (1H, d, J_{gem} = 11.4 Hz, C$\underline{H}_2$Bn), 4.60 (1H, d, J_{gem} = 11.4 Hz, C$\underline{H}_2$Bn), 4.47 (1H, d, J_{gem} = 11.4 Hz, C$\underline{H}_2$Bn), 4.21 (1H, d, $J_{\text{H2}′, \text{H3}′}$ = 1.2 Hz, H3′), 3.84 (1H, d, J_{gem} = 11.4 Hz, H5′), 3.76 (1H, d, J_{gem} = 11.4 Hz, H2′), 2.87 (1H, m, H2′), 2.48 (3H, s, S$\underline{C}$H₃), 2.29 (1H, m, H7′), 1.99 (3H, s, 5-C$\underline{H}_3$), 0.90 (3H, d, $J_{7′\text{-CH3, H7}′}$ = 7.2 Hz 7′-C$\underline{H}_3$); ¹³C NMR (150 MHz, CDCl₃) δ 213.8 ($\underline{C}$=S), 162.8 (C4), 148.9 (C2), 136.7 (aromatic), 136.0 (aromatic), 134.7 (C6), 127.6−126.7 (aromatic), 108.9 (C5), 88.3 (C4′), 87.8 (C1′), 81.1 (C3′), 78.7 (C6′), 72.8 ($\underline{C}$H₂Bn), 71.4 ($\underline{C}$H₂Bn), 65.3 (C5′), 46.4 (C2′), 29.6 (C7′), 18.1 ($\underline{C}$H₃S), 12.1 (7′-$\underline{C}$H₃), 11.7 (5-$\underline{C}$H₃); MALDI-TOF m/z [M + Na]⁺, found 591.163, calcd 591.160.

(1S,3R,4S,5S,7S)-7-Benzyloxy-1-benzyloxymethyl-5-methyl-3-(thymin-1-yl)-2-oxabicyclo[2.2.1]heptane (10) and (1R,3R,4S,5S,6S,7S)-5-Benzyloxy-6-benzyloxymethyl-7-methyl-3-(thymin-1-yl)-2-oxabicyclo[2.2.1]heptane (11). Compound **9** (130 mg, 0.230 mmol) was dissolved in dry toluene (6 mL) and purged with dry nitrogen for 30 min. AIBN (8.5 mg, 0.050 mmol) and n-Bu₃SnH (0.19 mL, 0.680 mmol) were added, and the reaction mixture was refluxed for 1.5 h. The mixture was cooled to rt. After evaporation of the solvent, the residue was chromatographed over silica gel (15−40% ethyl acetate in cyclohexane) to give compounds **10** (45 mg, 42%) and **11** (9 mg, 7%). **10**: ¹H NMR (500 MHz, CDCl₃) δ 8.79 (1H, s, N$\underline{H}$), 7.56 (1H, s, H6), 7.39−7.28 (10H, m, aromatic), 6.09 (1H, d, $J_{\text{H1}′, \text{H2}′}$ = 2.0 Hz, H1′), 4.74 (1H, d, J_{gem} = 10.0 Hz, C$\underline{H}_2$Bn), 4.65 (1H, d, J_{gem} = 10.0 Hz, C$\underline{H}_2$Bn), 4.59 (1H, d, J_{gem} = 10.0 Hz, C$\underline{H}_2$Bn), 4.58 (1H, d, J_{gem} = 10.0 Hz, C$\underline{H}_2$Bn), 4.06 (1H, s, H3′), 3.75 (1H, d, J_{gem} = 8.5 Hz, H5′), 3.72 (1H, d, J_{gem} = 8.5 Hz, H5″), 2.78 (1H, s, H2′), 2.02 (1H, dd, $J_{\text{H6}′, \text{H7}′}$ = 8.0 Hz, $J_{\text{H6}′, \text{H6}″}$ = 11.5 Hz, H6′), 1.96 (3H, s, 5-C$\underline{H}_3$), 1.70 (1H, m, H7′), 1.54 (1H, dd, $J_{\text{H6}′, \text{H7}′}$ = 4.0 Hz, $J_{\text{H6}′, \text{H6}″}$ = 11.5 Hz, H6″), 1.00 (3H, d, $J_{7′\text{-CH3, H7}′}$ = 6.0 Hz, 7′-C$\underline{H}_3$); ¹³C NMR (125 MHz, CDCl₃) δ 162.9 (C4), 148.9 (C2), 136.9 (aromatic), 136.6 (aromatic), 135.0 (C6), 127.4−126.6 (aromatic), 108.0 (C5), 88.6 (C1′), 88.2 (C4′), 81.3 (C3′), 72.7 ($\underline{C}$H₂Bn), 71.0 ($\underline{C}$H₂Bn), 66.8 (C5′), 46.9 (C2′), 37.4 (C6′), 22.7 (C7′), 19.8 (7′-$\underline{C}$H₃), 11.7 (5-$\underline{C}$H₃); MALDI-TOF m/z [M + Na]⁺, found 485.208, calcd 485.205. **11**: ¹H NMR (500 MHz, CDCl₃) δ 8.74 (1H, s, N$\underline{H}$), 7.41 (1H, s, H6), 7.31−7.19 (10H, m, aromatic), 5.80 (1H, s, H1′), 4.80 (1H, d, J_{gem} = 11.5 Hz, C$\underline{H}_2$Bn), 4.51 (1H, d, J_{gem} = 11.5 Hz, C$\underline{H}_2$Bn), 4.45 (1H, d, J_{gem} = 11.5 Hz, C$\underline{H}_2$Bn), 4.41 (1H, s, H6′), 4.35

(1H, d, J_{gem} = 11.5 Hz, C$\underline{H}_2$Bn), 4.27 (1H, dd, $J_{\text{H2}′, \text{H3}′}$ = 4.0 Hz, $J_{\text{H3}′, \text{H4}′}$ = 10.0 Hz, H3′), 3.69 (2H, d, H5′, 5″), 2.94 (1H, d, $J_{\text{H2}′, \text{H3}′}$ = 4.0 Hz, H2′), 2.52 (1H, m, $J_{\text{H3}′, \text{H4}′}$ = 10.0 Hz, $J_{\text{H4}′, \text{H6}′}$ = 1.5 Hz, H4′), 2.06 (1H, m, $J_{\text{H6}′, \text{H7}′}$ = 4.0 Hz, $J_{\text{H7}′, 7′\text{-CH3}}$ = 7.0 Hz, H7′), 1.88 (3H, s, 5′-C$\underline{H}_3$), 0.92 (3H, d, $J_{7′\text{-CH3, H7}′}$ = 7.0 Hz 7′-C$\underline{H}_3$); ¹³C NMR (125 MHz, CDCl₃) δ 163.1 (C4), 148.8 (C2), 137.5 (aromatic), 137.0 (aromatic), 135.1 (C6), 127.4−126.5 (aromatic), 108.0 (C5), 83.1 (C1′), 81.6 (C6′), 73.6 (C3′), 72.5 ($\underline{C}$H₂Bn), 70.5 ($\underline{C}$H₂Bn), 64.9 (C5′), 47.7 (C2′), 40.8 (C4′), 36.4 (C7′), 11.7 (5-$\underline{C}$H₃), 8.9 (7′-$\underline{C}$H₃); MALDI-TOF m/z [M + H]⁺, found 463.219, calcd 463.223.

General Procedure for Phosphoramidite Synthesis. To a solution of substrate (1 equiv) in dry dichloromethane were added DIPEA (6 equiv) and 2-cyanoethyl N,N-diisopropyl phosphoramidochloridite (3 equiv) dropwise in an ice bath. The reaction was allowed to warm to rt and stirred at this temperature for 3 h. After being quenched with methanol, the mixture was diluted by dichloromethane, washed with saturated NaHCO₃ solution, dried over MgSO₄, and concentrated. The residue was subjected to short column chromatography on silica gel to give phosphoramidite, which was first precipitated in n-hexane and then dried over P₂O₅ on vacuum for 3 days before it was used for DNA synthesis.

Oligonucleotide Synthesis and Purification. All AONs were synthesized using an automated DNA/RNA synthesizer based on phosphoramidite chemistry. For native A, G, and C building block, fast deprotecting phosphoramidites (Ac for C, iPr-Pac for G, Pac for A) were used. Standard DNA synthesis reagents and cycle were used except that 0.25 M 5-[3,5-bis(trifluoromethyl)phenyl]-1*H*-tetrazole (activator 42) was used as the activator and Tac₂O as the cap A. For incorporation of modified nucleotides, extended coupling time (10 min comparing to 25 s for native nucleotides) was used. For AONs **2−9**, the deprotections were carried out in 33% aqueous NH₃ for 72 h at 55 °C (the longer deprotection times were used to ensure complete removal of the Tol group). Other oligoes (AONs **1** and **10−21**) were deprotected at room temperature by treatment with 33% aqueous NH₃ for 12 h. After deprotection, all crude oligos were purified by denaturing PAGE (20% polyacrylamide with 7 M urea), extracted with 0.3 M NaOAc, and desalted with a C-18 reverse phase cartridge to give AONs in >99% purity, and correct masses have been obtained by MALDI-TOF mass spectroscopy for each of them.

RNA was also synthesized by a solid-supported phosphoramidite approach based on the 2′-O-TEM strategy.[68,69]

UV Melting Experiments. Determination of the T_m of the AON/RNA hybrids or AON/DNA duplex was carried out in the following buffer: 60 mM Tris-HCl (pH 7.5), 60 mM KCl, 0.8 mM MgCl₂. Absorbance was monitored at 260 nm in the temperature range from 20 to 65 °C using a UV spectrophotometer equipped with a Peltier temperature programmer with the heating rate of 1 °C/min. Prior to measurements, the samples (1 μM of AON and 1 μM complementary DNA or RNA mixture) were preannealed by heating to 80 °C for 5 min followed by slow cooling to 21 °C and 30 min equilibration at this temperature. The value of T_m is the average of two or three independent measurements. If error of the first two measurements is > ±0.3 °C, the third measurement was carried out to check if the error is indeed within ±0.3 °C; otherwise, it is repeated.

CD Spectroscopy. CD spectra were recorded from 300 to 200 nm in 0.2 cm path length cuvettes. Spectra were obtained with an AON/RNA or AON/DNA duplex concentration of 10 μM in

(68) Zhou, C; Honcharenko, D.; Chattopadhyaya, J. *Org. Biomol. Chem.* **2007**, *5*, 333−343.
(69) Zhou, C.; Pathmasiri, W.; Honcharenko, D.; Chatterjee, S.; Barman, J.; Chattoapdhyaya, J. *Can. J. Chem.* **2007**, *85*, 293−301.

60 mM Tris-HCl (pH 7.5), 60 Mm KCl, 0.8 mM MgCl$_2$. All spectra were measured at 20 °C, and each spectrum is an average of five experiments from which the CD value of the buffer was subtracted.

^{32}P Labeling of Oligonucleotides. The oligoribonucleotides and oligodeoxyribonucleotides were 5′-end-labeled with ^{32}P using T4 polynucleotide kinase, [γ-^{32}P]ATP, and the standard protocol. Labeled AONs and the target RNA were purified by QIAquick Nucleotide Removal Kit, and specific activities were measured using a Beckman LS 3801 counter.

SVPDE Degradation Studies. Stability of the AONs toward 3′-exonucleases was tested using phosphodiesterase I from *Crotalus adamanteus* (obtained from USB Corporation, Cleveland, OH). All reactions were performed at 3 μM DNA concentration (5′-end ^{32}P-labeled with specific activity 80 000 cpm) in 100 mM Tris-HCl (pH 8.0) and 15 mM MgCl$_2$ at 21 °C. An exonuclease concentration of 6.7 ng/μL was used for digestion of oligonucleotides. Total reaction volume was 30 μL. Aliquots (3 μL) were taken at proper time points and quenched by addition of stop solution (4 μL) [containing 0.05 M EDTA, 0.05% (w/v) bromophenol blue, and 0.05% (w/v) xylene cyanole in 80% formamide]. Reaction progress was monitored by 20% denaturing (7 M urea) PAGE and autoradiography.

Stability Studies in Human Blood Serum. AONs at 2 μM concentration (5′-end ^{32}P-labeled with specific activity 80 000 cpm) were incubated in 10 μL of human blood serum (male AB, obtained from Sigma-Aldrich) at 21 °C (total reaction volume was 36 μL). Aliquots (3 μL) were taken at proper time points and quenched with 4 μL of stop solution [containing 0.05 M EDTA, 0.05% (w/v) bromophenol blue, and 0.05% (w/v) xylene cyanole in 80% formamide], resolved in 20% polyacrylamide denaturing (7 M urea) gel electrophoresis and visualized by autoradiography.

RNase H Digestion Assay. Target 0.1 μM RNA (specific activity 80 000 cpm) and AON (2 μM) were incubated in a buffer containing 20 mM Tris-HCl (pH 7.5), 20 mM KCl, 10 mM MgCl$_2$, 0.1 mM EDTA, and 0.1 mM DTT at 21 °C in the presence of 0.01 U *E. coli* RNase H (obtained from USB Corporation, Cleveland, OH). Prior to the addition of the enzyme, reaction components were preannealed in the reaction buffer by heating at 80 °C for 5 min followed by slow cooling to 21 °C and 30 min equilibration at this temperature. Total reaction volume was 30 μL. Aliquots of 3 μL were removed after 5, 10, 15, 30, and 60 min, and the reactions were terminated by mixing with stop solution [containing 0.05 M EDTA, 0.05% (w/v) bromophenol blue, and 0.05% (w/v) xylene cyanole in 80% formamide]. The samples were subjected to 20% 7 M urea PAGE and visualized by autoradiography. Pseudo-first-order reaction rates could be obtained by fitting the digestion curves to single-exponential decay functions.

Supporting Information Available: ^{1}H, ^{13}C, ^{31}P, DEPT, COSY, HMQC, HMBC of α-L-carba-LNA derivatives (part I); 1D NOE spectra, ^{1}H homo or double decoupling spectra of key intermediates **5a**, **5b**, **8a**, **8b**, **8c**, **10**, **11**, **19**, **21**, **15a**, **15b**, and **15c** (part II); autoradiograms of 20% denaturing PAGE as well as degradation curves, showing the cleavage kinetics of target RNA in AON/RNA hybrids by *E. coli* RNase H1; synthesis and NMR characterization of intermediates **5b**, **6b**, **7b**, **12b**, **13b**, **15b**, **13c**, **15c**, **17**, **18**, **19**, **21** as well as the characterization for final amidites **16a**, **16b**, **16c**, and **22** (part II); chemical models of AON/RNA hybrids containing one α-L-carba-LNA or β-D-carba-LNA modification (part II). This material is available free of charge via the Internet at http://pubs.acs.org.